



Published in final edited form as:

*J Med Chem.* 2022 March 24; 65(6): 4403–4423. doi:10.1021/acs.jmedchem.1c01577.

## Boosting the Discovery of Small Molecule Inhibitors of Glucose-6-Phosphate Dehydrogenase for the Treatment of Cancer, Infectious Diseases, and Inflammation

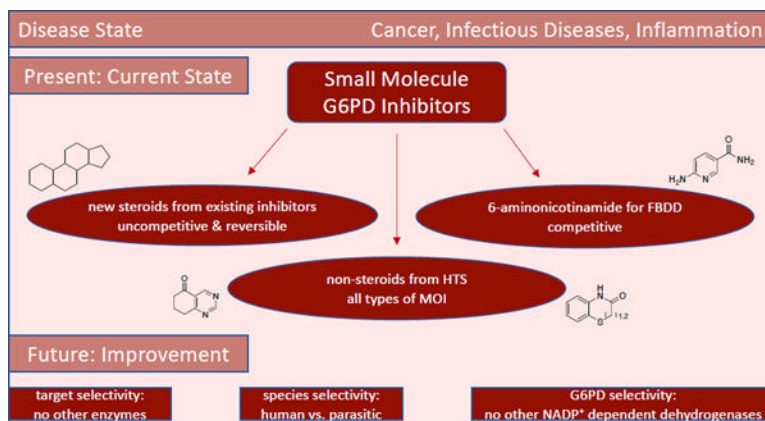
Ana Koperniku<sup>1,\*</sup>, Adriana A. Garcia<sup>1</sup>, Daria Mochly-Rosen<sup>1</sup>

<sup>1</sup>Department of Chemical and Systems Biology, School of Medicine, Stanford University, 269 Campus Dr, Stanford, CA 94305, USA

### Abstract

We present an overview of small molecule glucose-6-phosphate dehydrogenase (G6PD) inhibitors that have potential for use in the treatment of cancer, infectious diseases, and inflammation. Both steroidal and non-steroidal inhibitors have been identified, with steroidal inhibitors lacking target selectivity. The main scaffolds encountered in non-steroidal inhibitors are quinazolinones and benzothiazinones/benzothiazepinones. Three molecules show promise for development as anti-parasitic (**25** and **29**) and anti-inflammatory (**32**) agents. Regarding modality of inhibition (MOI), steroidal inhibitors have been shown to be uncompetitive and reversible. Non-steroidal small molecules have exhibited all types of MOI. Strategies to boost the discovery of small molecule G6PD inhibitors include exploration of structure-activity relationships (SARs) for established inhibitors, employment of high-throughput screening (HTS), and fragment-based drug discovery (FBDD) for the identification of new hits. We discuss the challenges and gaps associated with drug discovery efforts of G6PD inhibitors from *in silico*, *in vitro* and *in cellulo* to *in vivo* studies.

### Graphical Abstract



\*Corresponding Author: Ana Koperniku, annkope@stanford.edu.

**Author Contributions:** A.K. drafted the manuscript and A.K., A.A.G. and D.M-R. edited it. All authors have approved of the final version.

We declare no competing interests.

## Keywords

small molecules; inhibitors; drug discovery; cancer; infectious diseases; inflammation

---

## Introduction

Glucose-6-phosphate dehydrogenase (G6PD) catalyzes the conversion of glucose-6-phosphate (G6P) to 6-phospho-glucono- $\delta$ -lactone (6PGL), the first and rate-limiting step in the oxidative phase of the pentose phosphate pathway (PPP) (Figure 1). Production of NADPH in this transformation allows for glutathione disulfide (GSSG) to be reduced to the monomeric thiol, glutathione (GSH). In turn, GSH acts as a radical scavenger and prevents the accumulation of reactive oxygen species (ROS).<sup>1-2</sup> The NADPH generated in this process can be used for fatty acid synthesis<sup>3-4</sup> whereas ribose-5-phosphate (R-5P), the isomer of ribulose-5-phosphate (Ru-5P) and open form to the respective furanose, is important for nucleotide synthesis.<sup>1, 5-7</sup>

Given the vital role of G6PD in nucleic acid synthesis, fatty acid synthesis, and redox homeostasis, G6PD is a compelling target for modulation. Indeed, hypoactive or hyperactive G6PD has been linked to the pathology of many human diseases, including cancer,<sup>8-10</sup> hemolytic anemia,<sup>11</sup> type II diabetes,<sup>12-13</sup> cardiovascular diseases,<sup>14-17</sup> and neurodegenerative diseases.<sup>18-19</sup> In the cases of hemolytic anemia and neurodegenerative disorders, the pathology is caused by reduced G6PD activity and activation of G6PD is of therapeutic interest; an activator of G6PD would mitigate oxidative stress derived from underperforming G6PD. However, in the context of cancer and chronic inflammation, G6PD is hyperactive and requires inhibition. Additionally, the activity of parasitic G6PD, present in parasites that cause trypanosoma or malaria, is critical for parasitic survival and the inhibition of parasitic G6PD has been explored as a treatment against infectious diseases. This Perspective focuses on the discovery and potential development of small molecule inhibitors of G6PD and their use in cancer, infectious diseases, and chronic inflammation.

## Steroidal G6PD Inhibitors in the Context of Cancer and Infectious Diseases: Optimization of Existing Inhibitors via SAR Exploration

### Cancer

The history of G6PD inhibitors as potential therapeutics for cancer treatment starts with dehydroepiandrosterone (DHEA) (**1**) and epiandrosterone (EA) (**2**) (Figure 2). Both DHEA (**1**) and EA (**2**) are involved in the metabolic pathway of testosterone, with EA having a weaker androgenic activity compared to DHEA. There are three enzymes for which DHEA (**1**) serves as a substrate in its naturally occurring role: 3- $\beta$ -hydroxysteroid dehydrogenase 2 (HSD3B2), 17- $\beta$ -hydroxysteroid dehydrogenase 5 (17BHSD5), and steroid sulfatase (sulfotransferase). Sulfotransferases introduce sulfate groups to hydroxy groups, rendering DHEA and other substrates more water soluble. Given that **1** is involved in testosterone biosynthetic pathways,<sup>20-21</sup> it is apparent that lack of target selectivity has raised concerns for its consideration as an anticancer agent.

Marks and Banks were the first to show that 17- and 20-ketosteroids act as inhibitors of mammalian G6PD.<sup>22</sup> Over the years, mechanistic investigations have demonstrated that **1** acts as an uncompetitive inhibitor of G6PD with respect to both NADP<sup>+</sup> and G6P.<sup>23</sup> The  $K_M$  for both the substrate and NADP<sup>+</sup> or the products (lactone and NADPH) across different studies, confirm uncompetitive inhibition ( $K_{M,G6P} \sim 6K_{M,NADP^+}$  and  $K_{M,lactone} \sim 35K_{M,NADPH}$ ).<sup>23–25</sup> Additionally, the reported  $K_i$  values for the forward and reverse reactions suggest reversible inhibition, implying uncompetitive, yet reversible, inhibition of G6PD by **1** and related steroids.<sup>23</sup> This type of inhibition for both NADP<sup>+</sup> and G6P indicates that it binds to the ternary enzyme-NADP<sup>+</sup>-G6P complex.<sup>26</sup> Although there have been studies to propose this MOI, since a co-crystal structure of the steroid/G6PD/NADP<sup>+</sup> complex is not available, the pharmacophoric interactions which may inform drug design remain unknown. Crystal structures of human (*Homo sapiens*; tetrameric),<sup>27–28</sup> trypanosomal (*Trypanosoma cruzi*; tetrameric),<sup>29</sup> and bacterial (*Leuconostoc mesenteroides*; dimeric)<sup>30–31</sup> G6PD will assist in analyzing pharmacophoric interactions and will help inform future SAR studies.

In recent years, the groups of Hamilton and Cordeiro have focused on the development of steroidal analogues of **1** and **2** with the goal of improving selectivity for G6PD. Although both groups have focused on the identification of new steroidal analogues, their drug discovery approaches have been different. The Hamilton group has focused on targeting human G6PD (hG6PD) for cancer and the Cordeiro group has targeted trypanosoma (TrG6PD) to selectively inhibit the parasite G6PD as a treatment for trypanosomiasis.

Hamilton *et al.*<sup>32</sup> classified the newly designed and synthesized analogues into three categories: androstane analogues with 3 $\beta$ -amino-substituents (**3**), pregnane analogues with 3 $\beta$ -amino-substituents (**4**) and androstane derivatives with 3 $\alpha$ -amino-substituents (**5**), as summarized in Figure 2. Of the three G6PD inhibitory analogues, the last class of analogues **5** (3 $\alpha$ -analogues) showed inferior inhibitory activity compared to **1** and **2**, highlighting the importance of retaining the R group above the ring (3 $\beta$ -analogues **3** and **4**). Replacement of the 3-OH with other hydrogen donors such as amides, ureas, carbamates, sulfamides and sulfonamides led to analogues with superior activity (Figure 2). From the 3 $\beta$ -androstane analogues, urea **3a** and sulfamide **3b** demonstrated up to 10-fold higher inhibitory activity compared to **1** and **2**, with IC<sub>50</sub> values of  $1.0 \pm 0.1 \mu\text{M}$  (R = NHCONHEt, urea **3a**) and  $1.2 \pm 0.1 \mu\text{M}$  (R = NHSO<sub>2</sub>NH<sub>2</sub>, sulfamide **3b**), respectively.

Of the 3 $\beta$ -pregnane derivatives, the corresponding sulfamide **4a** (R = NHSO<sub>2</sub>NH<sub>2</sub>) inhibits the enzyme with an IC<sub>50</sub> of  $1.2 \pm 0.2 \mu\text{M}$ . The presence of a hydroxy group at C21 proved to be essential for this higher potency; in its absence, the IC<sub>50</sub> was increased to  $2.0 \pm 0.4 \mu\text{M}$ . However, this replacement provided a five-fold more potent analogue compared to the parent **1** and **2**. As shown in Figure 2, the groups on the C3 carbon serve as hydrogen bond donors and the groups at C17 (androstane core) or C20 (pregnane core) act as hydrogen bond acceptors. Compounds which demonstrated better activity than the parent **1** and **2** in the enzyme assay (IC<sub>50</sub> <  $9.4 \pm 1.0 \mu\text{M}$ ) were tested in cellular assays using HEK293T cells. Unfortunately, the pharmacologic profile of the selected compounds was poor and no correlation between the enzymatic and cellular assays could be drawn.

Two main factors may influence the lack of biological activity: aqueous solubility and cell permeability. Two of the most potent compounds with excellent inhibitory enzyme activity, 3 $\beta$ -sulfamides **3b** and **4a**, were water-soluble; however, they were the least potent in cellular assays. Therefore, poor aqueous solubility does not explain discrepancies between *in vitro* and *in cellulo* potency. To determine whether membrane permeability explained reduced compound activity, a Caco-2 permeability assay was employed. The measured permeabilities were good to moderate, suggesting poor permeability does not cause reduced inhibitory activity in cell-based assays. The authors concluded that a combination of factors pertinent to solubility, permeability and inherent assay differences are the cause for the observed discrepancy in inhibitory activities. However, it is possible that since these compounds are structurally similar to **1**, they could be sequestered by enzymes recognizing **1** (HSD3B2, 17BHSD5 and sulfotransferase) or be metabolically transformed in cellular assays and, thus, their actual intracellular concentration is insufficient to inhibit G6PD. *In vitro* studies using human liver microsomes demonstrated good metabolic stability for the compounds, making it unlikely for metabolic transformations catalyzed by P450 enzymes to account for the profile discrepancy observed between the biochemical and assay in cells.

### Infectious Diseases

Although research efforts have focused on the development of new steroidal analogues of both **1** and **2** to improve target selectivity between the cognate protein and G6PD in humans, differences in sequence conservation across species have made it an attractive target for the treatment of infectious diseases, by selectively targeting the G6PD enzyme of the pathological microorganisms. Steroidal derivatives of **1** and **2** have been shown to exert anti-infective properties in the parasites *Plasmodium falciparum* (*P. falciparum*),<sup>33</sup> *Cryptosporidium parvum*,<sup>34</sup> *Schistosoma mansoni*,<sup>35</sup> *Trypanosoma cruzi* (*T. cruzi*),<sup>36</sup> *Taenia crassiceps*<sup>37</sup> and *Entamoeba histolytica*.<sup>38</sup> In all cases, the mechanism of action is unknown. In the case of *Trypanosoma* species, steroidal derivatives have been investigated for development as anti-infective agents.

In the work developed by Cordeiro, **1** and **2** (Figure 2) inhibited TrG6PD,<sup>39</sup> acting as uncompetitive inhibitors for both substrates, G6P and NADP<sup>+</sup> (in the low micromolar range), providing trypanocidal activity against *Trypanosoma brucei* (*T. brucei*). Notably the  $K_i$  for TrG6PD was ~6-fold lower than that for hG6PD for both G6P and NADP<sup>+</sup>, indicating a higher affinity of both steroids **1** and **2** for the parasitic G6PD. Viability assays on cultures of bloodstream forms of *T. brucei* (427 strain) identified an LD<sub>50</sub> for **1** and **2** of 43.8  $\pm$  2 and 24.5  $\pm$  0.7  $\mu$ M, respectively. Both **1** and **2** were also tested against *Leishmania mexicana* (*L. mexicana*) but had no inhibitory effect. These results demonstrate that **1** and **2** may be selective for certain types of trypanosomes. The molecular basis for this difference may shed light on the pharmacophore or its pharmacokinetics in the two trypanosome species.

In a subsequent study, Cordeiro *et al.* showed that 16-bromoepiandrosterone (16-BrEA, **6**) (Figure 2) exerts trypanocidal activity against *T. cruzi*, the parasitic protozoan causing Chagas disease, *via* the inhibition of TrG6PD.<sup>40</sup> The IC<sub>50</sub> value for **6** was 86  $\pm$  8 nM and its LD<sub>50</sub> in parasitic cultures (*T. cruzi* epimastigotes, Y strain) was found to be 12  $\pm$  8  $\mu$ M, with this 100-fold value difference suggesting that **6** has a broad therapeutic index. For

comparison, the authors measured the  $IC_{50}$  values of **1** and **2** for TrG6PD which were found to be  $25.0 \pm 3.5$  and  $5.6 \pm 1.2$   $\mu\text{M}$ , respectively. Whereas the authors measured the  $K_i$  values for **1** ( $K_i = 21.5 \pm 0.5$   $\mu\text{M}$ ) and **2** ( $K_i = 4.8 \pm 0.3$   $\mu\text{M}$ ), the measurement of the  $K_i$  value of **6** would have allowed for a broad comparison across the species *T. cruzi* and *T. brucei*, and potency comparison for hG6PD, since this comparison was addressed in the study focusing on *T. brucei*.<sup>39</sup> Notably, the same group has further increased the selectivity for TrG6PD (*T. cruzi*) by designing and synthesizing derivatives of **6** and achieving high selectivity for the parasitic G6PD.<sup>41</sup> In addition to maintaining the bromine at C16, the C3-hydroxy group was either esterified or etherified. This strategy, leading to abolition of hydrogen bond donating features of the C3-hydroxy group, aimed to increase the selectivity of the new compounds for TrG6PD over hG6PD.

The necessity for C3-hydrogen bond donating groups was projected as an essential feature for inhibitory activity toward hG6PD by Hamilton *et al.* Non-brominated derivatives were also synthesized for some analogues. Although these non-brominated derivatives were not cytotoxic to the host, they were not potent inhibitors of *T. cruzi*. This further demonstrates the necessity for bromine at C16 for optimal potency against the parasite. In Figure 3, we show C3 esterified and etherified derivatives of type **7** and **8**, respectively. These compounds were tested in rat H9C2 rat cardiomyocytes infected with epimastigotes (Y strain) of *T. cruzi*. Compounds of type **7** and **8** that at a concentration of 20  $\mu\text{M}$  reduced the cell viability to 25% or less were subjected to a dose-response assay starting at lower concentrations. The purpose was to measure efficacy against the parasite and toxicity against the host cell. In addition, the selectivity index (SI) ( $EC_{50\text{-host}}/EC_{50\text{-}T.\text{cruzi}}$ ) was measured to assess selectivity between the TrG6PD and hG6PD. Carboxylic esters **7a** and **7b** were shown to be the least potent ( $EC_{50}$  values  $8.5 \pm 1.5$  and  $16.7 \pm 4.2$   $\mu\text{M}$ , respectively); however, **7b** had the broader therapeutic window between the parasite and the host ( $EC_{50}$  value for the host for **7b**:  $54 \pm 3.3$   $\mu\text{M}$ ). On the other hand, sulfonate **7c** and ether derivatives **8a-c** were more potent (range of  $EC_{50}$  values:  $\sim 2\text{--}4$   $\mu\text{M}$ ) against *T. cruzi* but insufficient selectivity was achieved between the parasite and the host. A reason for the discrepancy in potency between the carboxylate esters and the ether derivatives could also be that the esters are cleaved by esterases in the cytosol, therefore, a greater dose is required to achieve the same pharmacological profile compared to the ether derivatives. Although compounds **7b** and **8c** had nearly the same SI, the  $EC_{50}$  for **8c** was as low as  $8.5 \pm 1.9$   $\mu\text{M}$  for the host, rendering it cytotoxic. Future development for preclinical studies would need to focus on increasing the SI through additional rounds of SAR optimization and evaluation of the amine congeners of **8b** and **8c** for optimal dissolution in the stomach; amines, in contrast to amides, can be protonated and that contributes to their better solubility. Although optimal dissolution depends on protonation of the molecule, the determinant for absorption is the availability of the uncharged molecule, that is, the free base. Unless the internalization mechanism involves organic anion or cation transporters, only the free base is permeable through cell membranes *via* diffusion. Other non-brominated analogues of **2** with non-hydrolyzable groups at C3 but which possess substituents with hydrogen bond donating or accepting groups were in general weak inhibitors of TrG6PD.

An advantage associated with all steroidal inhibitors, encountered both in the context of cancer and infectious diseases, is that they lack functional groups which would serve as Michael acceptors. Thus, their promiscuity as substrates for Michael donors, such as thiolates from cysteines, is attenuated. Despite **1** and **2** exhibiting lower  $K_i$  values for TrG6PD (for *T. brucei*) compared to hG6PD and **6** exhibiting a lower  $IC_{50}$  value compared to **1** and **2** for *T. cruzi*, the lack of selectivity for parasitic G6PD can cause complications in the mammalian host. These complications are due to the androgenic effects of steroids.<sup>42–43</sup>

## Non-Steroidal G6PD Inhibitors from HTS in the Context of Infectious Diseases, Cancer, and Inflammation

### Infectious Diseases

The lack of species and target selectivity led Cordeiro *et al.* to pursue non-steroidal G6PD inhibitors that are selective toward the protozoic G6PD enzyme by conducting high throughput screening.<sup>44</sup> Hits identified in the primary screen and their analogues were subjected to follow-up studies; compounds that inhibited TrG6PD between 40% and 100% at 20  $\mu$ M were subjected to dose-response for  $IC_{50}$  determination. Those compounds with  $IC_{50}$  values of  $0.48 < IC_{50} < 32 \mu$ M were grouped into two chemical categories: thienopyrimidines **9** and quinazolinones **10** (Figure 4).

SAR studies with the thienopyrimidines **9** revealed that the amido group at the C6 position of the core was required for the expression of inhibitory activity and long chain hydrophobic aliphatic substituents at the *N*-3 position are required in order to observe inhibitory activity in the low micromolar range. Compound **9a** was found to be the most potent inhibitor with an  $IC_{50}$  of  $4.9 \pm 0.5 \mu$ M. The replacement of the long chains with shorter or more hydrophilic chains reduced the potency.

Regarding the second class, quinazolinones **10**, it was shown that the carbonyl at C5 was essential for inhibitory activity. The presence of the methyl group at C4 increased selectivity toward TrG6PD and it should be noted that the most potent compound in this series, quinazolinone **10a**, ( $IC_{50}$ :  $0.48 \pm 0.05 \mu$ M) lacked the methyl group ( $R^2 = H$  instead of  $CH_3$ ), highlighting that potency does not guarantee selectivity. The presence of bulky substituents  $R^3/R^4$  at C7 of the nucleus proved detrimental for inhibitory activity, resulting in a dramatic increase in the  $IC_{50}$  values. Finally, the SAR analysis for C2 of the quinazolinone ring implied that the amine attached at that position can either be an aniline (a weakly basic, electron deficient, nitrogen atom) or a piperazine (a more basic, electron rich nitrogen atom). Notably, the piperazine linker between the quinazolinone moiety and the aromatic ring in **10b** delivered a highly selective compound for TrG6PD over hG6PD ( $IC_{50}$ :  $0.61 \pm 0.05$  vs.  $>80 \mu$ M, respectively).

The most potent compounds from each category are uncompetitive, reversible inhibitors of TrG6PD, as was the case for all steroidal TrG6PD inhibitors (Figure 4). In addition, these compounds compete with **2** for binding to the target enzyme, suggesting that non-steroidal and steroidal compounds are binding to the same region in TrG6PD.<sup>45–46</sup>



The authors used these compounds in tests with epimastigote forms of *T. cruzi*, Y strain, and classified the compounds in accordance with the percentage of remaining viable cells. Although thienopyrimidine **9a** was the most active against recombinant TrG6PD, it had no effect on cell viability. The most active compounds in the viability assay stemmed from the quinazolinone class, with **10a** being the most active in the *in vitro* biochemical assay and exhibiting comparable activity to benznidazole ( $8.5 \pm 1.5 \mu\text{M}$  for **10a**,  $10 \pm 0.8 \mu\text{M}$  for benznidazole) against epimastigotes *T. cruzi*. Other quinazolinones bearing a methyl group at C4 ( $R^2 = \text{CH}_3$ ) and a *para*-fluoro ( $R^1 = \text{F}$ ) or a *meta*-methyl ( $R^1 = \text{CH}_3$ ) substituent on the aniline exhibited even lower  $\text{EC}_{50}$  values than benznidazole in the viability assay, providing an anchor for the development of potential trypanocidal agents. Thienopyrimidines **9** have a pyrimidinone moiety whereas quinazolinones **10** have a pyrimidine heterocycle as part of their scaffold, suggesting that the pyrimidine nitrogens in both cases may play a role in the pharmacophoric interactions with the target. However, the presence of the primary amide group in thienopyrimidines confers significant polarity to the molecules. This indicates that the thienopyrimidine series requires further optimization, most likely *via* the introduction of lipophilic substituents on the amido nitrogen to achieve translatable activity from *in vitro* to *in vivo* assays.

Although co-crystal structures for human or trypanosomal G6PD with an inhibitor bound do not exist, the crystal structures of both, including substrates and co-factors, allow for comparison between the two and can guide drug discovery efforts (Figure 5). Both hG6PD (PDB ID 2BH9) and TrG6PD (PDB ID 5AQ1) have a catalytic site for the substrate (G6P) and co-factor ( $\text{NADP}^+$ ). However, only the mammalian hG6PD has an additional  $\text{NADP}^+$ -binding site, known as the structural or allosteric  $\text{NADP}^+$ -binding site, which determines long term protein stability and structural integrity of the enzyme.

By overlaying hG6PD and TrG6PD crystal structures, we show the point-by-point amino acid comparison for each G6PD species, with emphasis placed on ligand-binding sites. There are three key differences between the two that can be exploited for selectivity of one over the other. Two are found at the structural  $\text{NADP}^+$ -binding site. At this site, Arg487 in hG6PD is replaced by Cys528 in TrG6PD. An antimalarial compound that covalently interacts with the TrG6PD cysteine may allow for selectivity between the human and *Trypanosoma* G6PD. In addition, Lys366 in hG6PD is Leu409 in TrG6PD, thus in the latter case, the interactions between an envisioned inhibitor and that residue would be limited to hydrophobic. Thus, Cys528 and Leu409 found in *Trypanosoma* can be exploited as targets for cross-linking with small molecules or hydrophobic interactions, respectively.

The third difference between the two structures is at the catalytic  $\text{NADP}^+$ -binding site; Tyr147 in hG6PD is Phe191 in TrG6PD. Although both residues are aromatic, their orientation is almost perpendicular to each other. A plausible explanation is that the phenolic OH from Tyr147 acts as a H-bond donor toward the OH of the ribose (H-bond acceptor) attached to the pyridinium ring of the co-factor ( $\text{NADP}^+$ ). This structural difference has the potential to be considered for the design of competitive  $\text{NADP}^+$  inhibitors selective for each species. Regarding the catalytic G6P site, it is nearly identical between each species and selective competitive inhibitors for G6P is less likely.

Another parasite for which non-steroidal G6PD inhibitors have been developed is *P. falciparum*, the parasite that causes malaria. Different from the hG6PD, *P. falciparum* contains a bifunctional chimeric enzyme, composed of both G6PD and 6-phosphoglucono- $\delta$ -lactonase (6PGLase), (PfGluPho), which together catalyze the first and second step of the PPP (Figure 1).<sup>47–48</sup> The amino acid sequence for 6PGLases is well conserved across species;<sup>49</sup> however, the G6PD sequence has a 62 residue insertion at the *N*-terminus relative to hG6PD, and this insertion is conserved in other *Plasmodium* species.<sup>47–50</sup> This conserved sequence, present only in the parasite, can potentially be used for the discovery of selective antimalarial drugs. However, the C-terminus of PfGluPho is homologous to the other G6PDs, which may present a challenge for drug discovery.

The Bode group used a library screen to identify new antimalarial agents that inhibit PfGluPho.<sup>51</sup> Four major classes of commercially available compounds were identified based on their core: pyrimidinones **11**, quinazolinones **12**, chromenones **13**, and sulfonamides **14** (Table 1). Pyrimidinetrienes **11a–c** (pyrimidinedione **11d**) and quinazolinones **12a–b** showed appreciable inhibitory activity toward recombinant PfGluPho [IC<sub>50</sub> range: (4.5 ± 1.6)–(19.9 ± 7.2)  $\mu$ M]. In *in vitro* *P. falciparum* culture assays (3D7 strain), chromenone **13a** and sulfonamides **14a–b** suppressed the viability of the parasite with IC<sub>50</sub> values ranging from (0.97 ± 0.15)–(5.3 ± 2)  $\mu$ M. The same compounds also inhibited recombinant PfGluPho, with **13a** being at least a 10-fold more potent inhibitor compared to **14a–b** in the biochemical assay (Table 1).

To assess time-dependence and reversibility, the authors measured different IC<sub>50</sub> values following the protocol of: 1 h pre-incubation and 1 h post-dilution (1:1), 1 h preincubation and 0 h post-dilution (1:0), and 0 h pre-incubation and 0 h post-dilution (0:0). The last experimental arrangement corresponds to the control experiment. If there was a decrease in the IC<sub>50</sub> value after pre-incubation (1:0) compared to the control (0:0), the inhibition occurred in a time-dependent manner. If there was a decrease in the IC<sub>50</sub> value after pre-incubation and post-dilution (1:1) compared to the control (0:0), the inhibition was irreversible. If the IC<sub>50</sub> value remained the same after pre-incubation and post-dilution, the inhibition was reversible.

Compound **13a** had an IC<sub>50</sub> value of (1.1 ± 0.4)–(1.5 ± 0.4)  $\mu$ M regardless of whether it was subject to pre-incubation or post-dilution conditions. Similarly, for **14a** and **14b**, the IC<sub>50</sub> values were >30  $\mu$ M regardless of whether or not the compound was pre-incubated with the PfGluPho enzyme. After post-dilution, the IC<sub>50</sub> for **14a** decreased to 22 ± 8  $\mu$ M but remained unchanged for **14b**. Regarding translatability, the most potent compounds identified in the biochemical assay did not suppress the viability of the *Plasmodium*. This may reflect chemical or enzymatic instability of the compound; the duration of the biochemical assay was 20–30 min whereas the *in vitro* assay with *Plasmodium* culture (3D7 strain) was 72 h.

All of these PfGluPho inhibitors exhibit mixed kinetics for inhibition of G6P and are non-competitive or competitive with NADP<sup>+</sup>. Reversibility of inhibition was observed for **11c** and **11d** since the IC<sub>50</sub> values were recovered after post-dilution (Table 1). Compounds **12a** and **12b** exhibited mixed-type of inhibition of G6P and were non-competitive with NADP<sup>+</sup>.



In addition, similar  $K_i$  values after post-dilution were obtained and these compounds were found to be irreversible inhibitors. Notably, **12a** and **12b** lack functionalities with which they would covalently bind to the target.

As was the case for trypanosomiasis, the above compounds were tested for selectivity using the recombinant hG6PD; only **13a** was more potent toward PfGluPho (Table 1), regardless of pre- and post-dilution times ( $IC_{50}$  values:  $1.1 \pm 0.4$  or  $1.5 \pm 0.4$   $\mu\text{M}$  for PfGluPho and  $2.2 \pm 0.7$  or  $2.6 \pm 0.7$   $\mu\text{M}$  for hG6PD). Moreover, when both human cells and the parasite species were present in the culture, compound **13a** demonstrated an enhanced inhibitory activity on parasitic growth, with  $IC_{50}$  values in the low  $\mu\text{M}$  range ( $IC_{50} = 0.97 \pm 0.15$   $\mu\text{M}$ ) (Table 1). In contrast, compounds **14a** and **14b** inhibited recombinant hG6PD in a time-dependent manner; the  $IC_{50}$  value fell from  $>30$   $\mu\text{M}$  to  $0.4 \pm 0.0$  and  $0.6 \pm 0.0$   $\mu\text{M}$ , respectively, after pre-incubation. In addition, these values remained in the same range after post-dilution, suggesting irreversibility of inhibition. Although these latter compounds targeted the G6PD element of *Plasmodium* PfGluPho, species selectivity was not observed.

Of the four categories of compounds **11–14** presented in Table 1, classes **12** and **13** are less promiscuous and, therefore, present as the preferred vehicles to consider for “hit to lead” optimization. The promiscuity of compounds **11** lies in their functionality which presents Michael acceptors that are activated by two carbonyl moieties (*vide infra*). The scaffold of pyrimidine-2,4,6(1*H*,3*H*,5*H*)-trione is present in barbiturates and this structural feature may cause off-target effects; barbiturates elicit their sedative effect by acting on GABA<sub>A</sub> receptors in the mammalian central nervous system. However, what renders barbiturates active is the appropriate substitution at the carbon between the two carbonyl functionalities.<sup>52</sup> In the projected structures **11a-c** (Figure 6), that carbon is substituted with an alkylidene moiety and, therefore, the resulting acrylamide moiety renders the molecules as potential Michael acceptors. Upon exposure to GSH or cysteine, compounds of type **15** can be obtained, suggesting the potential to react with cysteines present in G6PD. GSH cellular concentrations range from 0.1 to 10 mM,<sup>53–54</sup> a range that ensures the presence of sufficient GSH even if minor portions of it are depleted by Michael acceptors. Regarding class **14**, the presence of the *p*-aminophenol skeleton poses the risk for oxidation to the corresponding sulfonated parabenzoquinone imines **16**. These benzoquinone imines **16** are potent Michael acceptors and can be captured by thiolates to deliver products **17**. This is the pathway observed for paracetamol metabolism and rationalizes the administration of *N*-acetylcysteine as an antidote in case of paracetamol poisoning. *N*-acetylcysteine can be converted into cysteine in the blood. Thus, it can provide a cysteine source for GSH biosynthesis or the liberated cysteine directly cross-couple with *N*-acetyl-*p*-benzoquinone imine which is the metabolite of paracetamol.<sup>55</sup>

In a study focusing on the chemical genetics of *P. falciparum*, **18** (ChemDiv: C276–1187) and **19** (ChemDiv: D052–0147) (Figure 7a) were shown to selectively target the 6PGLase part in PhGluPho.<sup>56</sup> Compound **18** is a quinolinone (shown in blue, Figure 7a), which is structurally similar to the quinazolinone chemotype **10** (Figure 4, Table 1). However, it was later shown that **18** inhibited both PfGluPho and hG6PD, as did the above compounds.<sup>57</sup> Regarding its chemical reactivity, **18** is an enamionone and, thus, its properties as a Michael acceptor are attenuated.

In contrast to compounds **11**, **14** (once oxidized to **16**, Figure 6) and **18**, which are prone to undergoing two-electron transfer reactions with intracellular components, **19** is a structural alert for a single electron transfer reaction.<sup>58</sup> Concerns surrounding this structural alert problem may explain the absence of follow up studies with **19**. Specifically, after reduction intermediate **20** transfers a single electron to molecular oxygen to form superoxide ion ( $O_2^{\bullet-}$ ) and the radical intermediate **21** (Figure 7b). Intermediate **21** is oxidized back to **19** with concomitant release of hydrogen peroxide ( $H_2O_2$ ). This redox cycling activity is characteristic of pyrimidinetriazinediones (PTDs); other examples include toxoflavin **22** and 2-methyl-ferulenone **23**. A necessity for these reactions to occur *in vitro* is the presence of strong reducing agents in the buffers, such as dithiothreitol (DTT) or tris(2-carboxyethyl)phosphine.<sup>59</sup> Assays to evaluate such reactivity include measurement of released hydrogen peroxide *in vitro* and ATP depletion in cells. Assays based on the fluorescent signal of resorufin have been employed for the segregation of well-performing caspase-8 and cathepsin L inhibitors from false-positive hits.<sup>60</sup>

A strategy to circumvent this activity upon SAR optimization is to replace the PDT nitrogen atom of the triazine core, which is reduced prior to the generation of the radical intermediates, with a carbon atom (compounds of type **24**, Figure 7c). In that case the triazine ring is replaced by a pyridazine ring.

The most successful study identifying a selective PfGluPho small molecule inhibitor was that conducted by the Bode group.<sup>61</sup> Starting with a HTS campaign that evaluated 350,000 compounds at a concentration of 20  $\mu M$ , a promising cluster of benzothiazinone derivatives was identified, with five leading to further SAR studies. In all assays, hG6PD was used as a counter-assay to ensure specificity for PfGluPho. Essential structural features for inhibitory activity toward PfGluPho included: 1) a basic alkylamine as part of the side chain of the amide; 2) an unsubstituted nitrogen of the benzothiazinone ring; and 3) an unaltered sulfur on the benzothiazinone ring (Figure 8). A series of analogues was synthesized that included substituent variation on the styryl ring and the amido nitrogen. Further SAR on the styryl ring substituents did not lead to a dramatic shift in inhibitory potency; however, the styryl ring was a necessity for inhibitory activity. 2-Aminomethyl pyrrolidine substituents on the amido nitrogen increased the potency. Stereochemical evaluation of the 2-aminomethyl pyrrolidines showed that the (*R*)-enantiomer was 8-fold higher in potency than the (*S*)-enantiomer, delivering **25** as the most potent of all of the analogues studied ( $IC_{50}$ :  $0.9 \pm 0.0 \mu M$ ), and was specific for PfGluPho. It exhibited mixed inhibition kinetics with  $NADP^+$  but was competitive with G6P. Given that **25** bears the Michael accepting acrylamide moiety, the authors prudently performed a GSH-based assay to measure levels of remaining compound upon exposure to GSH. The data showed that the levels of **25** remained intact upon exposure to GSH (ethacrynic acid was used as positive control). According to the protocol used, the ratio of [compound]:[GSH] was 1:5 and the final GSH concentration was 50  $\mu M$ . The concentration ratio is a fixed ratio and does not reflect the ratio observed once the drug is internalized in the cell in all cases. The value of 50  $\mu M$  for GSH concentration is much lower than the concentration range observed in the cytosol in cells (0.1–2 mM in most cell types, 10 mM in hepatocytes).<sup>53–54</sup> Indeed, if **25** remains intact in the presence of a five-fold excess of GSH, the conjecture is that its levels will be

not be perturbed in the presence of GSH in cellular or in *in vivo* studies. When bioactive compounds are Michael acceptors, a GSH-based assay is essential, as it determines their potential for further drug development, a general strategy for consideration in the field of covalent inhibitors in medicinal chemistry.<sup>62–63</sup>

Compound **25** was subjected to *in vitro* pharmacological studies to evaluate absorption, distribution, metabolism, excretion, and toxicity (ADMET). Compound **25** was highly permeable across artificial models of cell membranes. The presence of the amino groups allows for its protonation in the low pH environment of the stomach, contributing to its solubility. However, only the free base can be subsequently absorbed. A parallel artificial membrane model assay (PAMPA) was used to show its high permeability under conditions of increased pH in the donor compartment. Membrane models resembling the blood-brain barrier (BBB) were used to demonstrate high permeability. In addition, **25** was shown to be highly plasma protein bound which will influence the brain bioavailability of the compound. An assay using Fa2N-4 immortalized human hepatocytes was performed to show that **25** is not toxic under these conditions. Compound **25** was further evaluated in *P. falciparum* cultures *in vitro* using chloroquine-sensitive (3D7 strain, IC<sub>50</sub>: 2.3 ± 0.2 μM) and chloroquine-resistant (Dd2 strain, IC<sub>50</sub>: 3.7 ± 0.9 μM) strains. The same group performed studies in parasitic cultures in previous studies.<sup>51</sup>

In contrast to the *Trypanosoma* parasite, there are no G6PD crystal structures available for any of the *Plasmodium* species. However, Alencar *et al.*, used the hG6PD structure to build a homology model for PfGluPho.<sup>64</sup> A key difference between hG6PD and PfGluPho was the replacement of Arg365 (hG6PD) with Asp370 (PfGluPho). Given that **25** exhibits competitive inhibition for substrate G6P in biochemical assays and was selective for PfGluPho, the authors docked **25** in the G6P binding site of PfGluPho, which was superimposed to the hG6PD crystal structure (PDB ID 2BHL) with G6P bound. This led the authors to synthesize a series of G6P analogues.

Given that **25** is a competitive inhibitor of G6P and against the backdrop of the Arg365→Asp370 mutation, the authors hypothesized that the protonated amino group of **25** interacts with Asp370, an interaction that they illustrated by docking it in the G6P binding site. Building further on this hypothesis and focusing on G6P, the authors envisioned, synthesized, and evaluated a series of G6P analogues. In these G6P analogues, the phosphate group at C6 was replaced by a thioether (**26**) or groups acting as hydrogen bond donors or acceptors, including sulfones **27** and sulfonamides **28**. In addition, a terminal amino, cyano or guanidino group was placed after the interjection of an alkyl chain. The alkyl chain filled the empty space between what would be Arg365 (hG6PD) to the existing Asp370 (PfGluPho) whereas the protonated amino or guanidino groups were projected to form ionic interactions with the carboxylate moiety of Asp370 (Figure 9).

*In vitro* evaluation of the compounds showed that indeed compounds bearing either the amino or guanidino group (**26a**, **26c**, **28a**, n = 1, Figure 9) had higher affinity for PfGluPho compared to the compounds with the cyano group. In addition, based on the SI measured for the *K<sub>i</sub>* for G6P [SI: ratio *K<sub>i</sub>*hG6PD/*K<sub>i</sub>*PfGluPho], the same compounds were more selective for PfGluPho. Notably, **26a** exhibited 26-fold selectivity for PfGluPho compared

to hG6PD. The internal substitution at C6 also affects affinity, with the compounds bearing sulfonamides showing the highest affinity and thioethers the lowest (**28a**>**27a**>**26a**, **28b**>**27b**>**26c**).

Despite the broad therapeutic index for a few of these compounds, the IC<sub>50</sub> values obtained from treatment of parasitic cultures were in the range of sub- to low millimolar, presumably owing to the high polarity of the compounds as sugar analogues. The compounds were also tested in the human hepatoma HepG2 cell line at a concentration ranging from 0.2 to 2 mM. Even at the highest concentration of 2 mM, none of the compounds impacted cell viability by more than 30%.

Another avenue of research would be to develop small molecules which are not analogues of G6P but are based on the projected pharmacophore between **25** and the PfGluPho; non-glucoside molecules may have an enhanced profile in the phenotypic assays due to their greater lipophilic character. Nonetheless, the authors projected a potential pharmacophoric interaction of **25** with the target and a plausible rationale for its selectivity toward PfGluPho compared to hG6PD. Overall, the data for the non-glucosidic **25** and glucosidic analogues **26–28** provide an anchor for their optimization or even for *de novo* design of other analogues.

GSSG, the oxidized form of GSH, inhibits PfGluPho.<sup>57</sup> Both the G6PD and 6PGLase domains of PhGluPho were inhibited as a function of *S*-glutathionylation of cysteine residues present in both domains. Except for Cys144, all of other cysteines reside in the G6PD domain of PfGluPho. In contrast, GSH (the reduced form of GSSG) and DTT increases the activity of the G6PD enzyme, but not the 6PGLase. DTT reverses the inhibition caused by *S*-glutathionylation of PhGluPho, indicating that the inhibition is reversible. Regarding the respective enzymes in humans (hG6PD and h6PGLase), it was shown that only h6PGLase was inhibited by GSSG. A plausible explanation for this phenomenon is that the PfGluPho has a region which is very similar to the GSH-binding site in GSH transferase.<sup>47</sup> This discrepancy in effect of GSSG suggests that it is a selective inhibitor of the G6PD domain of PhGluPho and hG6PD, and it could be considered as a potential therapeutic. However, as a hexapeptide, it is susceptible to proteolytic degradation when delivered into the blood. Notably, the monomeric GSH is not susceptible to peptidases/ proteases, compared to other peptides, because the peptide bond between the glutamate and the amino group of cysteine is formed at the  $\gamma$ -COOH instead of  $\alpha$ -COOH. However, this bond can only be hydrolyzed by  $\gamma$ -glutamyltranspeptidase.<sup>65</sup> This resistance may prove beneficial for GSSG delivery but may need additional optimization. As well as being a peptide, GSSG is a disulfide and, thus, it can participate in thiol exchange reactions with off-target free cysteines.<sup>66</sup> This poses a second limitation for its consideration as a therapeutic agent. The sequence difference identified recently between the human (Arg) and the parasite (Glu) has allowed for the design of scaffolds, using molecular modeling methods, which selectively inhibit PhGluPho.<sup>67</sup> The authors reported that they are currently examining how to capitalize on this information.

In addition to *S*-glutathionylation, *S*-nitrosation mediated by nitrosated GSH is another modification that can inhibit the activity of the enzyme. In contrast to what was shown in the

previous work by Jortzik *et al.*, Haeussler *et al.* showed that the G6PD part of PfGluPho and PvGluPho (Pv: *Plasmodium vivax*, *P. vivax*) are hardly affected by these post-translational modifications, with *S*-nitrosation leading to only minor changes in enzyme activity.<sup>68</sup>

As well as examining the effect of these post-translational modifications on enzymatic activity, the authors determined the effect of amino acid substitution of the PfGluPho sequence on activity. Three of these mutations are naturally occurring within the PfGluPho gene (S315Y, L395F, F507L) whereas two of them included serine substitution at positions 899 and 900 to examine effect of phosphorylation, another post-translational modification, on enzymatic activity. Interestingly, these substitutions have minimal effects on enzymatic activity and substrate affinities compared to wild-type PfGluPho. Notably the double serine sequence at positions of 899–900 is specific and highly conserved to *Plasmodium* species. Taking advantage of the differences in amino acid residues across different species (parasitic *vs.* human) through protein engineering, may be a strategy for developing selective chemical probes for a given species, as was the case for **25**. This strategy is known as site-directed drug discovery.<sup>69</sup>

In addition to **25**, which selectively inhibits PfGluPho over hG6PD, **29** had the same selectivity profile for PfGluPho, was even more potent (IC<sub>50</sub>: ~190 nM)<sup>70</sup> and was also potent against PvG6PD (IC<sub>50</sub>: 15.3 ± 0.9 μM) (Figure 10).<sup>68</sup> This study highlights the importance of achieving two aims at once: the discovery of a compound selective for the G6PD belonging to different genera (*Plasmodium vs.* human) and the possibility of one compound to be efficacious across the species of the same genus (*P. falciparum* and *P. vivax*). Superimposition of **25** and **29** validates the stringent requirement for the (*R*)-stereochemistry on the side chain of amido nitrogen (Figure 10). The benzothiazinone ring has been expanded by one carbon to benzothiazepinone in **29** and fused with the aromatic ring instead of being connected with it *via* an alkylidene bridge as in **25**. This alters the relative orientation of the aromatic ring resulting in a more planar structure for **25** and a folded arrangement between thiazepinone and the aromatic ring for **29**. This second chemical probe validates the SAR and opens the road for further modifications in the benzothiazinone or benzothiazepinone ring. Since both compounds are competitive inhibitors for G6P, this can be guided by docking both at the substrate binding site and thoroughly examining the pharmacophore with G6PD.

## Cancer

Except for **25** and **29**, which showed promising selectivity, the lack of selectivity observed for the rest of the compounds between the parasitic and hG6PD has inspired research groups to shift their focus to hG6PD inhibitors which target cancer and inflammation. Bode and co-workers screened 50,000 compounds at a concentration of 5 μg/mL and identified 107 that inhibit hG6PD by 50%.<sup>71</sup> The five hG6PD inhibitors **12a-b**, **14a**, **30**, **31** (Table 2) demonstrated IC<sub>50</sub> values of < 4 μM and were selected for follow up studies. Among these five compounds, four of them (**12a-b**, **14a**, **31**) were previously reported to inhibit PfGluPho. In Table 2, we present the IC<sub>50</sub> values for PfGluPho and hG6PD for comparison.

Compounds **12a** and **12b** incorporate the common quinazolinone nucleus highlighted in blue. In a prior study by Bode, **12b** was tested in both biochemical and parasitic assays but was found to be a potent inhibitor of PfGluPho only in the biochemical assay. The other three compounds **14a**, **30**, **31** are structural alerts, either because they may engage in redox cycling activity (**14a**) or act as a Michael acceptor (**30** and **31** where the 1,4-conjugated moiety is shown in teal). Compound **14a** can generate the phenoxy radical which can react with superoxide ion (as in Figure 7b) and be oxidized to a benzoquinone imine of type **16** which is a Michael acceptor (Figure 6).

The forms of inhibition by these five compounds were then determined. Initial dose-response experiments to calculate IC<sub>50</sub> values, in which pre-incubation was used without post-dilution (to examine reversibility), placed **14a** as the most potent inhibitor with an IC<sub>50</sub> of 0.4 ± 0.0 μM and **30** as the least potent inhibitor with an IC<sub>50</sub> of 3.1 ± 0.8 μM (Table 2). Inhibition of hG6PD by sulfonamide **14a** was irreversible; its effect was not diminished following post-dilution.<sup>51</sup> Furthermore, the IC<sub>50</sub> was 100-fold lower after pre-incubation relative to no pre-incubation conditions. Compounds **12a**, **12b** and **31** are competitive inhibitors for G6P and showed a mixed type of inhibition for NADP<sup>+</sup>, with **31** showing both mixed type and non-competitive inhibition for NADP<sup>+</sup>. Compound **30** is also an inhibitor that is competitive for both G6P and NADP<sup>+</sup>. Notably, **12a** and **12b** inhibited hG6PD with a different kinetic signature compared to PfGluPho; for PfGluPho these inhibitors exhibited a mixed-type of inhibition with respect to G6P and were non-competitive with NADP<sup>+</sup> (see under non-steroidal inhibitors, infectious diseases). This difference in inhibitory signature can serve as anchor to develop selective competitive inhibitors based on **12a** and **12b** for G6P for hG6PD.

Except for **12b**, the remaining 4 compounds were tested in cell-based assays. Two cell lines were used: MCF10-A, used as a control, and the tumorigenic IMCF10-AT1 cell line. Compounds **12a**, **30** and **31** had no effect on cell growth, with this being attributed to low membrane permeability or adhesion to other biomolecules. Sulfonamide **14a** was the sole compound to demonstrate a measurable IC<sub>50</sub> of 25 μM for the tumorigenic cell line compared to the >50 μM observed for the control cell line. This is another example where the GSH-based assay should have been performed,<sup>61</sup> to validate that the inhibitory effect of **14a** is not due to direct reaction between **16** with thiolates from free cysteines *via* a Michael addition, as shown in Figure 6.

Up to this point, we have discussed the selectivity of the identified inhibitors for G6PD from different species. In the context of cancer, another selectivity issue to consider is the selectivity towards the malignant cells relative to healthy cells. For these inhibitors to be further developed as anticancer agents, they must selectively act on malignant cells otherwise there is a risk of triggering hemolytic anemia to subjects. There are several means to improve such selectivity, including nano-formulation-based delivery using either passive targeting, which relies on the enhanced retention and permeability of cancerous tissues, or active targeting.<sup>72</sup> Active targeting employs the functionalization of the nanoparticles surface for targeted delivery to the desired tissue.



In addition to targeting G6PD in humans for the treatment of cancer, another enzyme which is distinct from the cytosolic G6PD is hexose-6-phosphate dehydrogenase (H6PD). H6PD resides in the endoplasmic reticulum and catalyzes both the first and second step observed in the PPP; that is the conversion of G6P to 6-phosphogluconate (6PG) (Figure 1).<sup>73</sup> Like PfGluPho, H6PD contains a fusion protein of G6PD and 6PGLase. It is found predominantly in the liver and other tissues, but it is absent in red blood cells. It shares homology with hG6PD, is dimeric, and uses a different pool of NADP<sup>+</sup> as a cofactor compared to the cytosolic variant.<sup>74–76</sup> It was recently shown that H6PD plays an important role in breast and lung cancer by genetic inhibition<sup>77</sup> and, thereby, it can be considered for modulation using small molecules. Given that H6PD is absent in red blood cells, selective small molecule inhibitors for H6PD over hG6PD are compelling in that they will not cause hemolytic crises. However, the need for selective targeting of cancerous over healthy cells in all other tissues remains.

### Inflammation

The work of Cordeiro<sup>44</sup> that led to the identification of TrG6PD inhibitors served as an inspiration for the discovery of a hG6PD inhibitor by the Rabinowitz group.<sup>78</sup> This hG6PD inhibitor, G6PDi (**32**) (Figure 11), reduced NADPH levels in a variety of immune cell types, including T-cells, macrophages, and neutrophils. This corresponded to a decrease in cytokine production and oxidative bursts, in T-lymphocytes and neutrophils, respectively, revealing a role for G6PD in immune cells. G6PD is critical for normal immune cell function.<sup>79</sup> G6PD and the PPP have been associated with neuroinflammation,<sup>80</sup> and adipose tissue inflammation in obesity,<sup>81</sup> suggesting G6PD is a viable target for pathological inflammation.

In the context of drug discovery, **32** is an analogue of the quinazolinone **10c** (Figure 11), which was previously identified as a trypanosomal G6PD inhibitor,<sup>44</sup> and extensive chemistry optimization effort by Rabinowitz *et al.* resulted in the G6PD inhibitor **32** (Figure 11). The 3-methylaniline in **10c** was replaced by a 2-cyano-4-aminothiophene, while the cyclohexanone moiety has been replaced by cycloheptanone. Notably, the replacement of 2-cyano-4-aminothiophene by 3-aminobenzonitrile led to **33**, which had no effect on immune cells. Thus, **33** was used as a negative control in the studies. Compounds **32** and **33** differ in their 3D shape as shown by the structural overlay depicted in Figure 11. In addition, the substitution of H with a CH<sub>3</sub> on the nitrogen atom between the heterocycle and phenyl rings diminishes the hydrogen bond donating features in **33**. Therefore, even minimal structural changes can lead to dramatic activity shifts. In addition to the shift observed for species selectivity between **10c** and **32**, there was a shift in MOI. Although both agents exhibited reversible type of inhibition in the dilution assays, **10c** was shown to be uncompetitive for TrG6PD whereas **32** non-competitive for hG6PD. On the contrary, in the case of **12a** and **12b**, replacement of the methoxy group by a bromine and the benzene by a pyridine ring did not alter the selectivity for hG6PD over parasitic G6PD but **12b** was found to be more potent than **12a** for each species (Figure 11 & Table 2). In addition, the MOI was different for each species, as already addressed in this perspective. Overall, the preference for hG6PD informs SAR for the “hit to lead” phase to improve both preference and pharmacological effect.

The non-androgenic quinazolinones are a frequently encountered scaffold; they are found in inhibitors of inflammasomes associated with diabetes, cardiovascular and neurodegenerative diseases.<sup>82–83</sup> The quinazolinones also have anticancer agents, due to their inhibitory effects on inflammasomes formation<sup>82–83</sup> and tubulin polymerization.<sup>84–85</sup> Recently quinazolinones were found to be inhibitors of epoxide hydrolase, an enzyme targeted for blood pressure reduction, insulin sensitivity improvement and inflammation decrease.<sup>86</sup> Such a broad scope of applications suggests lower selectivity toward G6PD.

The work of Ramírez-Nava *et al.* identified four non-quinazolinone compounds with moderate inhibitory activity toward hG6PD.<sup>87</sup> Initial HTS led to 55 candidate compounds, four of which inhibited hG6PD activity by 40% at a concentration of 400  $\mu\text{M}$  (Figure 12a). Two of the four compounds, **34a** and **34b**, are homologues that contain a biphenyl ring and a phenylalkanoic group. The other two compounds, **35a** and **35b**, differ in the substitution of the aromatic ring (chloro for **35a** vs butoxy ring for **35b**). Although they share the 2-nitrothiazole ring with anti-protozoal nitazoxanide **35**, nitazoxanide **35** does not act through G6PD inhibition. In addition, the bridge between the headgroups in compounds **35a** and **35b** is a urea whereas in nitazoxanide the linker is an amide bond, a difference which impacts the 3D shape between them (Figure 12a). For all three compounds **35**, **35a**, and **35b**, the preferred conformation would be anticipated to involve the carbonyl oxygen from the amide or urea being oriented toward the sulfur of the nitrothiazole. As such, the non-bonding lone pair of the oxygen is able to engage with the  $\sigma^*$  antibonding orbital of sulfur, an interaction which confers stability to the system (Figure 12b).<sup>88</sup> This non-covalent interaction between sulfur and oxygen can be considered when further designing and optimizing drugs carrying this motif. Dose-response experiments showed that **35a** had the greatest inhibitory activity among the four compounds toward the recombinant hG6PD ( $\text{IC}_{50} = 121 \mu\text{M}$ ). Despite the structural similarities for the compound pairs of type **34** and **35**, the type of inhibition varied. Compounds **34a**, **34b**, and **35b** are non-competitive or uncompetitive inhibitors with respect to both G6P and  $\text{NADP}^+$ , whereas the most potent compound, **35a**, is a non-competitive inhibitor with respect to G6P and an uncompetitive inhibitor with respect to  $\text{NADP}^+$ . These differences in mechanism of inhibition suggest differences in the amino acids with which each of these compounds interact.

The study of Ramírez-Nava *et al.* also included molecular docking experiments. Although the projected inhibitors are weak, this is the first example of an *in silico* study in the history of non-steroidal G6PD inhibitors. For steroidal inhibitors, *in silico* studies of **6** and its analogues provided support for the selective effect of these compounds on the trypanosomal over hG6PD,<sup>89–90</sup> a trend observed by the group of Cordeiro in biochemical and cell-based assays. Using a blind docking protocol, Ramírez-Nava *et al.* the  $\Delta G$  free energies are consistent with the biochemical activities and suggested that the docking site for the compounds was either close to the catalytic or structural  $\text{NADP}^+$ , or near the binding of G6P. Compound **35a**, which was the most potent in the biochemical assays, had a  $\Delta G$  of  $-6.91 \text{ kcal/mol}$  at the structural  $\text{NADP}^+$  site, which was slightly higher when compared to the site near the G6P-binding site ( $-7.51 \text{ kcal/mol}$ ). However, it was considered more likely for inhibitor **35a** to enter the structural  $\text{NADP}^+$  region as it interacts with five out of the twelve amino acid residues involved in the binding of the structural

NADP<sup>+</sup>, despite the higher  $K_m$  observed for this binding. Such compounds that interact with the structural NADP<sup>+</sup> are important for selective inhibitory activity on hG6PD, as the structural NADP<sup>+</sup> site is absent in other dehydrogenases or parasitic G6PDs. Such *in silico* docking information by Ramírez-Nava *et al.* now provides potential grid boxes for future computational studies, as opposed to blind docking where the whole target represents the grid box.

A remarkable transition from steroidal to non-steroidal small molecules was the discovery of tamoxifen. The synthetic form of estradiol (**36**) is diethylstilbestrol (DES **37**), a derivative of *trans*-stilbene (Figure 13). The two phenolic oxygens in **37** are disposed at the same distance that phenolic oxygen at C3 and the hydroxy group at C17 exist in **36** and, like the prototype, **37** is an agonist.<sup>91</sup> This SAR subtended a rational approach for transitioning from the steroidal **36** to non-steroidal **37** which, at that time, was conducted in the absence of co-crystal structures. Tamoxifen **38** is a selective estrogen receptor modulator that acts as an antagonist in breast cancer cells but acts as an agonist in the uterus.<sup>92–93</sup> Both **37** and **38** possess the *trans*-stilbene core and the original synthetic agonist served as a scaffold to envision antagonists. Agonists such as **37**, stabilize helix 12 in the ligand binding domain and are fully engulfed in it. On the other hand, antagonists such as **38** that bear an additional bulky side chain cave into helices 3 and 11. This interjection prevents helix 12 in the receptor from adopting the agonist conformation and blocks recruitment of the coactivator to the ligand-binding site.<sup>94–95</sup> Similarly, it is expected upon unveiling the pharmacophoric interactions between G6PD and **1** or **2** that more knowledge will be available to refine the structure of small molecules obtained from HTS. The fact that similar structures arose from different screening strategies and cause similar biological activities adds to the confidence for the observed SAR to date.

The groups of Hamilton<sup>32</sup> and Cordeiro<sup>41</sup> have shown that hydrogen bond donors at C3 of the steroids are essential, and studies by Hamilton support the contention that hydrogen bond acceptors are necessary at C17. These data bring the discovery of non-steroidal G6PD molecules in the same perspective as for the identification of synthetic, non-steroidal estradiol agonists and antagonists, where groups at C3 and C17 were retained as part of the pharmacophore in the non-steroidal analogues (Figure 13).

We discussed earlier the interactions of hG6PD with co-factors and substrates, based on existing co-crystal structures that were used, guide structure-based drug design. In addition, we have highlighted the existing small molecule inhibitors that incorporate structural alerts which render them potentially unattractive candidates for lead optimization. These structural alerts include, but are not limited to, Michael acceptors and redox-cycling compounds. For Michael acceptors, promiscuity would be of concern but there are many Michael acceptors that are quite selective for their targets. In structure-based drug design, such moieties can be exploited under the premise that molecular recognition has been achieved between the target and the ligand structure. Molecular recognition, a concept and principle encountered primarily in supramolecular chemistry,<sup>96</sup> takes place *via* non-covalent interactions; these interactions are secondary interactions and assist with the localization of the drug in the target. Next, a Michael acceptor can be incorporated as a functional group for primary interaction to advance activity. Indeed, covalent drugs have gained ground in the recent

years,<sup>97–99</sup> using this dual strategy of molecular recognition and incorporation of a highly reactive, yet discriminating, moiety. A notable successful example based on this strategy includes the allosteric KRAS inhibitor, AMG510 **39**, which has an acrylamide moiety acting as Michael acceptor, yet it reacts specifically with Cys12 of the KRAS binding pocket (Figure 14).<sup>100–101</sup> This cysteine appears solely in mutated KRAS proteins present in cancerous cells and not in wild type KRAS (in wild type KRAS protein, position 12 is occupied by a glycine). Not only is pocket specificity achieved, but also selectivity between mutant and wild type isoforms, offering selectivity between cancerous and healthy cells, respectively.

Finally, although the crystal structure of the bacterial *L. mesenteroides* G6PD has been determined,<sup>30</sup> no agents or small molecules targeting the bacterial G6PD have been developed. This approach could open the road for new anti-bacterial agents and replace the current antibiotics, whose major liability is the resistance development. Suffice is to mention that selectivity for the bacterial G6PD over hG6PD will be essential for such inhibitors to be considered as antibiotics.

## Competitive G6PD Inhibitors for FBDD: Advantages and Disadvantages

In FBDD, the number of compounds which may be used for screening is in the range of a few thousands in contrast to HTS, where the number may reach many millions. Molecular weights of the compounds in FBDD are 150–200 Da and even millimolar affinities can prove useful in early stage of such a screen. Positive fragments need to then be grown (up to 500 Da) to optimize the compound and obtain nanomolar affinity. The translation of the fragment hit with weak affinities into the final drug lead can rely on *in silico* information (when crystal structure is available), but can be achieved also in its absence.<sup>102</sup> Initial fragments can also be grown through tethering of the fragments to the protein-binding site. This method introduces a disulfide bond between the fragment and a cysteine in a protein to stabilize the interactions, with the cysteine introduced in the target protein near the presumed binding site *via* mutagenesis.<sup>69, 103</sup>

The above methodologies can be applied, for example, on 6-aminonicotinamide (6AN, **40**), which inhibits G6PD competitively and its molecular weight is 137.14 (Figure 15).<sup>104</sup> However, **40** is not specific for G6PD since it competes for the binding of NAD<sup>+</sup> or NADP<sup>+</sup> of other dehydrogenases. Both a highly specific screen and computational docking of this fragment can identify a specific and high affinity lead.

Advantages of FBDD include the use of a smaller library and therefore the ability to use a more complicated assay, which might not be suitable for HTS. Following fragment screen, bioisosteric replacement leads to molecules with the improved and desired properties that are to be characterized and confirmed by orthogonal assays. A second advantage to begin with FBDD is that as the medicinal chemistry campaign begins with a fragment, there is a better chance of generating a small enough molecule with the desired pharmacological features. A disadvantage for FBDD is the reduced chemical space that is searched. However, the number of possible compounds that can be constructed from the original fragment is exponential, creating sufficient exploration of diverse chemical space. Another disadvantage

is the very weak interaction of the fragment with the target ( $K_d$  up to 5000  $\mu\text{M}$ ) requiring assays that are much more sensitive than those used in HTS. Although tethering, through disulfide bond to the target overcomes this limitation, it requires that all compounds in the fragment library to have a -SH group. It also requires quite extensive mutagenesis campaign of the target to identify the optimal cysteine mutant for the screen. Nevertheless, the lack of optimal and selective inhibitors for G6PD argues that more efforts in the field, including the use of FBDD should be employed.

### Summary and Outlook

In this perspective, we discussed small molecules which have been discovered and optimized for G6PD inhibition in the context of cancer, infectious diseases, and inflammation.

Candidate G6PD inhibitors can be classified into two major structural groups: steroidal and non-steroidal. Hamilton *et al.* and Cordeiro *et al.* presented their work on steroids with potential anticancer and trypanocidal activity, respectively. Their data suggest that hydrogen bond donors and acceptors at C3 and C17 of the steroids govern the SAR for potency and species selectivity. Despite the encouraging results regarding potency and species selectivity, the off-target androgenic effects pose a limitation for the development of these molecules as G6PD-targeting therapeutics.

In the case of non-steroidal small molecule G6PD inhibitors, the lack of species selectivity between the microorganism and hG6PD has served as an impetus for hit modification as an approach to the identification of species-selective G6PD antagonists. Three compounds stand out from the drug discovery efforts conducted to date and all are derived from HTS campaigns: the antimalarial compounds **25** and **29** and the anti-inflammatory agent **32**. Notably, inhibitor **32** evolved from optimization of trypanocidal agents that were introduced by the Cordeiro group. Although all three of these compounds have reached a degree of translatability in cellular and *in vivo* studies, their use in the clinic has yet to occur.

Non-steroidal G6PD inhibitors have been studied in the context of cancer using both biochemical and cellular assays; however, the lead inhibitors are structural alerts for either being Michael acceptors or for their redox cycling activity. *p*-Aminophenols of type **14** and PDT **19** are such examples. In addition, false positive hits can also stem from the conditions employed in biochemical assays; in the presence of super stoichiometric amounts of reductants and oxidants in buffer solutions, functional groups can be reduced or oxidized, respectively. Under physiological conditions these modifications would not occur. In cellular assays, enzyme metabolism and off-target cellular effects may account for false positive results. On the other hand, the polarity of the compounds and their consequent poor permeability creates a barrier for translation in cells or in *in vivo* studies and, thus, false negative results are obtained for *in cellulo* activity.

Regarding the structural alerts, there are *in vitro* assays that can evaluate the promiscuity of these ligands as Michael acceptors or redox cycling molecules; these assays measure the ability of the ligands to remain intact in the presence of free thiols, deplete GSH levels or produce  $\text{H}_2\text{O}_2$ , respectively. There are two solutions to address this substrate promiscuity during SAR optimization. The first one involves the structural modification in the part of the molecule responsible for reactivity (for example removal of the 1,4-conjugated system

in Michael acceptors or replacement of the triazine ring with diazine in flavone derivatives). Contrastingly, in the second strategy a highly reactive site is intentionally embedded in the molecule; however, promiscuity will need to be attenuated by judicious decoration of a molecule such that it is recognized by a specific pocket in the target.

Non-selective competitive inhibitors that inhibit several NADP<sup>+</sup>-dependent dehydrogenases, such as **40**, are also useful leads as they can provide a basis for *in silico* design, FBDD and medicinal chemistry efforts to increase their specificity for G6PD. The bar for selectivity is high in this case since there is already selectivity for a whole family of enzymes depending on the specific co-factor 6AN competes with (NADP<sup>+</sup> or NAD<sup>+</sup>). For that, in the case of FBDD, highly sensitive assays are required as opposed to HTS drug discovery, where specificity is the major factor governing subsequent SAR optimization.

A general challenge in the reports on the efforts to generate G6PD inhibitors is that IC<sub>50</sub> and not *K<sub>i</sub>* values are provided. IC<sub>50</sub> values are useful for biological evaluation; however, the values depend on the concentration of the enzyme used in the assay and, therefore, does not allow a comparison across other studies. In contrast, *K<sub>i</sub>* is an intrinsic parameter of each inhibitor; it depends on the equilibrium between the bound and unbound inhibitor, and, unlike IC<sub>50</sub>, it is independent of enzyme concentration. The shift from providing IC<sub>50</sub> to *K<sub>i</sub>* values is currently a practice but must become a mandate.

As the critical role of G6PD in a variety of human diseases becomes apparent, the field is now poised to address challenges and fill in gaps for the discovery of small molecule G6PD inhibitors. We anticipate this perspective will provide a platform to boost the discovery of target- and species-selective G6PD inhibitors for cancer, infectious diseases, inflammation, and other diseases in which G6PD plays a crucial role which is currently known or remains to be identified.

## ACKNOWLEDGMENT

A.K and D.M-R are supported by NIH R01 HD08442 awarded to D.M-R. A.A.G thanks the National Science Foundation for a Graduate Research Fellowship (NSF-GRFP) (Grant DGE 1656518) and National Institutes of Health (NIH) for a training grant (Grant 5T32GM113854).

### Funding Sources

The work was supported by R01 HD08442 to D.M-R., NSF-GRFP; A.A.G was supported in part by DGE 1656518 and 5T32GM113854.

## BIOGRAPHICAL SKETCHES

Ana Koperniku obtained her BSc in Pharmacy in 2011 and MSc in Pharmaceutical Chemistry in 2013 from National and Kapodistrian University of Athens. In 2013 she started at the University of British Columbia (UBC) as a PhD student and her doctoral thesis focused on the chemistry of *N*-silylated amines as precursors to diheteroarylamides and as substrates in transition metal catalyzed reactions to generate novel alkyl substituted amines in the groups of Profs. David Grierson and Laurel Schafer, respectively. She was an NSERC CREATE SusSyn and a Four-Year Doctoral Fellow at UBC. She is currently a PDF in the



Mochly-Rosen laboratory at Stanford University, where she is working on the identification of small molecule activators to correct enzymopathies.

Adriana A. Garcia received a B.S. in biochemistry from San Francisco State University. She is currently a graduate student in the department of Chemical and Systems Biology at Stanford University School of Medicine, in the lab of Daria Mochly-Rosen. She is a National Science Foundation – Graduate Research Fellowship Program (NSF-GRFP) fellow and her research uses biochemical and biophysical methods to study the structure-function relationship of clinically relevant mutations of a particular human enzymopathy. The goal of her studies is to identify therapeutic strategies that may correct protein structure and reduced enzymatic function caused by these mutations.

Daria Mochly-Rosen is a protein chemist in the Chemical and Systems Biology department at Stanford and leads a multi-disciplinary research lab focusing on the molecular mechanisms of diseases. She has published >300 articles and dozens of patents, was the Chair of her department, and the Senior Associate Dean for Research at Stanford University, School of Medicine. She is an expert in ‘translational research’ and through SPARK, a program she founded at Stanford in 2006, she helps shepherd scores of academic discoveries to licensing and clinical trials; >50% of the ~150 projects were licensed and/or entered clinical studies. Her lab’s research is focused on identifying peptide regulators of pathological protein-protein interactions and small molecules activators that correct common human enzymopathies; all as leads for drug discoveries.

## ABBREVIATIONS

<b>6PG</b>	6-phosphogluconate
<b>6PGL</b>	6-phosphoglucono- $\delta$ -lactone
<b>6PGLase</b>	6-phosphoglucono- $\delta$ -lactonase
<b>16-BrEA</b>	16-bromoepiandrosterone
<b>17BHSD5</b>	17- $\beta$ -hydroxysteroid dehydrogenase 5
<b>BBB</b>	blood-brain barrier
<b>C</b>	competitive
<b>Caco-2</b>	colorectal adenocarcinoma cell line 2
<b>DES</b>	diethylstilbestrol
<b>DHEA</b>	dehydroepiandrosterone
<b>DMF</b>	dimethylfumarate
<b>DTT</b>	dithiothreitol
<b>EA</b>	epiandrosterone

<b>Fa2N-4</b>	immortalized human hepatocytes line
<b>FBDD</b>	fragment-based drug discovery
<b>GABA<sub>A</sub></b>	gamma-amino-butyric acid-A
<b>G6PD</b>	glucose-6-phosphate dehydrogenase
<b>G6PDi</b>	glucose-6-phosphate dehydrogenase inhibitor
<b>GSH</b>	glutathione
<b>GSSG</b>	glutathione disulfide
<b>h</b>	hour
<b>H6PD</b>	hexose-6-phosphate dehydrogenase
<b>H9C2</b>	rat heart myocytes
<b>HepG2</b>	human hepatoma cells
<b>HEK293T</b>	human embryonic kidney cell line expressing antigen T
<b>hG6PD</b>	human glucose-6-phosphate dehydrogenase
<b>h6PGLase</b>	human 6-phosphoglucono- $\delta$ -lactonase
<b>HSD3B2</b>	3- $\beta$ -hydroxysteroid dehydrogenase 2
<b>hTERT</b>	human telomerase reverse transcriptase
<b>HTS</b>	high-throughput screening
<b>IC<sub>50</sub></b>	half maximal inhibitory concentration
<b>IDH</b>	isocitrate dehydrogenase
<b>Inc.</b>	incorporated
<b>LD<sub>50</sub></b>	median lethal dose
<b>M</b>	mixed-type
<b>MCF10-A</b>	non-malignant breast epithelial cell line
<b>MCF10-AT1</b>	pre-malignant breast epithelial cell line
<b>MOI</b>	modality of inhibition
<b>NC</b>	non-competitive
<b>NADP<sup>+</sup></b>	nicotinamide adenine dinucleotide phosphate
<b>NADPH</b>	reduced nicotinamide adenine dinucleotide phosphate
<b>PAMPA</b>	parallel artificial membrane permeability assay

<b>PDT</b>	pyrimidinetriazinedione
<b>PfGluPho</b>	Plasmodium falciparum glucose-6-phosphate dehydrogenase 6-phosphogluconolactonase
<b>P.falciparum</b>	Plasmodium falciparum
<b>P.vivax</b>	Plasmodium vivax
<b>PPP</b>	pentose phosphate pathway
<b>SAR</b>	structure-activity relationship
<b>SI</b>	selectivity index
<b>R-5P</b>	ribose-5-phosphate
<b>Ru-5-P</b>	ribulose-5-phosphate
<b>ROS</b>	reactive oxygen species
<b>T. cruzi</b>	Trypanosoma cruzi
<b>TrG6PD</b>	trypanosomal glucose-6-phosphate dehydrogenase
<b>vs.</b>	versus

## REFERENCES

1. Stanton RC, Glucose-6-phosphate dehydrogenase, NADPH, and cell survival. *IUBMB life* 2012, 64 (5), 362–369. [PubMed: 22431005]
2. Tian W-N; Braunstein LD; Pang J; Stuhlmeier KM; Xi Q-C; Tian X; Stanton RC, Importance of Glucose-6-phosphate Dehydrogenase Activity for Cell Growth. *J. Biol. Chem* 1998, 273 (17), 10609–10617. [PubMed: 9553122]
3. Agrawal PK; Canvin DT, The pentose phosphate pathway in relation to fat synthesis in the developing castor oil seed. *Plant Physiol* 1971, 47 (5), 672–675. [PubMed: 16657682]
4. Hutchings D; Rawsthorne S; Emes MJ, Fatty Acid Synthesis and the Oxidative Pentose Phosphate Pathway in Developing Embryos of Oilseed Rape (*Brassica napus* L.). *J. Exp. Bot* 2004, 56 (412), 577–585. [PubMed: 15611146]
5. Kornberg A; Horecker BL; Horecker BL; Smyrniotis PZ, [42] Glucose-6-phosphate dehydrogenase 6-Phosphogluconic Dehydrogenase. In *Methods in Enzymology*, Academic Press: 1955; Vol. 1, pp 323–327.
6. Gao J; Aksoy BA; Dogrusoz U; Dresdner G; Gross B; Sumer SO; Sun Y; Jacobsen A; Sinha R; Larsson E; Cerami E; Sander C; Schultz N, Integrative Analysis of Complex Cancer Genomics and Clinical Profiles Using the cBioPortal. *Sci. Signal* 2013, 6 (269), p11. [PubMed: 23550210]
7. Cerami E; Gao J; Dogrusoz U; Gross BE; Sumer SO; Aksoy BA; Jacobsen A; Byrne CJ; Heuer ML; Larsson E; Antipin Y; Reva B; Goldberg AP; Sander C; Schultz N, The cBio Cancer Genomics Portal: an Open Platform for Exploring Multidimensional Cancer Genomics Data. *Cancer Discov* 2012, 2 (5), 401–404. [PubMed: 22588877]
8. Li R; Wang W; Yang Y; Gu C, Exploring the Role of Glucose-6-phosphate Dehydrogenase in Cancer. *Oncol. Rep* 2020, 44 (6), 2325–2336. [PubMed: 33125150]
9. Khan A; Siddiqui S; Husain SA; Mazurek S; Iqbal MA, Phytochemicals Targeting Metabolic Reprogramming in Cancer: An Assessment of Role, Mechanisms, Pathways, and Therapeutic Relevance. *J. Agric. Food Chem* 2021, 69 (25), 6897–6928.

10. Cho ES; Cha YH; Kim HS; Kim NH; Yook JI, The Pentose Phosphate Pathway as a Potential Target for Cancer Therapy. *Biomol. Ther* 2018, 26 (1), 29–38.
11. Beutler E, G6PD Deficiency. *Blood* 1994, 84 (11), 3613–36. [PubMed: 7949118]
12. Gaskin RS; Estwick D; Peddi R, G6PD Deficiency: its Role in the High Prevalence of Hypertension and Diabetes Mellitus. *Ethn. Dis* 2001, 11 (4), 749–754. [PubMed: 11763298]
13. Heymann AD; Cohen Y; Chodick G, Glucose-6-Phosphate Dehydrogenase Deficiency and Type 2 Diabetes. *Diabetes Care* 2012, 35 (8), e58–e58. [PubMed: 22826451]
14. Vimercati C; Qanud K; Mitacchione G; Sosnowska D; Ungvari Z; Sarnari R; Mania D; Patel N; Hintze TH; Gupte SA; Stanley WC; Recchia FA, Beneficial Effects of Acute Inhibition of the Oxidative Pentose Phosphate Pathway in the Failing Heart. *Am. J. Physiol. Heart Circ. Physiol* 2014, 306 (5), H709–H717. [PubMed: 24414069]
15. Meloni L; Manca MR; Loddo I; Cioglia G; Cocco P; Schwartz A; Muntoni S; Muntoni S, Glucose-6-phosphate Dehydrogenase Deficiency Protects Against Coronary Heart Disease. *J. Inherit. Metab. Dis* 2008, 31 (3), 412–417. [PubMed: 18392752]
16. Hecker PA; Lionetti V; Ribeiro RF Jr.; Rastogi S; Brown BH; O'Connell KA; Cox JW; Shekar KC; Gamble DM; Sabbah HN; Leopold JA; Gupte SA; Recchia FA; Stanley WC, Glucose 6-phosphate Dehydrogenase Deficiency Increases Redox Stress and Moderately Accelerates the Development of Heart Failure. *Circ. Heart Fail* 2013, 6 (1), 118–126. [PubMed: 23170010]
17. Chhabra A; Mishra S; Kumar G; Gupta A; Keshri GK; Bharti B; Meena RN; Prabhakar AK; Singh DK; Bhargava K; Sharma M, Glucose-6-phosphate Dehydrogenase is Critical for Suppression of Cardiac Hypertrophy by H<sub>2</sub>S. *Cell Death Discov* 2018, 4 (1), 6.
18. Tang BL, Neuroprotection by Glucose-6-phosphate Dehydrogenase and the Pentose Phosphate Pathway. *J. Cell. Biochem* 2019, 120 (9), 14285–14295. [PubMed: 31127649]
19. Jeng W; Loniewska MM; Wells PG, Brain Glucose-6-phosphate Dehydrogenase Protects against Endogenous Oxidative DNA Damage and Neurodegeneration in Aged Mice. *ACS Chem. Neurosci* 2013, 4 (7), 1123–1132. [PubMed: 23672460]
20. Webb SJ; Geoghegan TE; Prough RA; Michael Miller KK, The Biological Actions of Dehydroepiandrosterone Involves Multiple Receptors. *Drug. Metab. Rev* 2006, 38 (1–2), 89–116. [PubMed: 16684650]
21. Turcu A; Smith JM; Auchus R; Rainey WE, Adrenal Androgens and Androgen Precursors- definition, Synthesis, Regulation and Physiologic Actions. *Compr. Physiol* 2014, 4 (4), 1369–1381. [PubMed: 25428847]
22. Marks PA; Banks J, Inhibition of Mammalian Glucose-6-Phosphate Dehydrogenase by Steroids. *Proc. Natl. Acad. Sci* 1960, 46 (4), 447–452. [PubMed: 16590626]
23. Gordon G; Mackow MC; Levy HR, On the Mechanism of Interaction of Steroids with Human Glucose-6-phosphate Dehydrogenase. *Arch. Biochem. Biophys* 1995, 318 (1), 25–29. [PubMed: 7726568]
24. Beutler E; Kuhl W, Characteristics and Significance of the Reverse Glucose-6-phosphate Dehydrogenase Reaction. *J. Lab. Clin. Med* 1986, 107 (6), 502–507. [PubMed: 3711719]
25. Bautista JM; Mason PJ; Luzzatto L, Purification and Properties of Human Glucose-6-phosphate Dehydrogenase Made in *E. coli*. *Biochim. Biophys. Acta* 1992, 1119 (1), 74–80. [PubMed: 1540638]
26. Cornish-Bowden A, Why is Uncompetitive Inhibition so Rare? *FEBS Lett* 1986, 203 (1), 3–6. [PubMed: 3720956]
27. Au SWN; Gover S; Lam VMS; Adams MJ, Human Glucose-6-phosphate Dehydrogenase: The Crystal Structure Reveals a Structural NADP<sup>+</sup> Molecule and Provides Insights into Enzyme Deficiency. *Structure* 2000, 8 (3), 293–303. [PubMed: 10745013]
28. Kotaka M; Gover S; Vandeputte-Rutten L; Au SW; Lam VM; Adams MJ, Structural Studies of Glucose-6-phosphate and NADP<sup>+</sup> Binding to Human Glucose-6-phosphate Dehydrogenase. *Acta Crystallogr. D* 2005, 61 (5), 495–504. [PubMed: 15858258]
29. Mercaldi GF; Dawson A; Hunter WN; Cordeiro AT, The Structure of a Trypanosoma Cruzi Glucose-6-phosphate Dehydrogenase Reveals Differences from the Mammalian Enzyme. *FEBS Lett* 2016, 590 (16), 2776–2786. [PubMed: 27391210]

30. Rowland P; Basak AK; Gover S; Levy HR; Adams MJ, The Three-dimensional Structure of Glucose 6-phosphate Dehydrogenase from *Leuconostoc mesenteroides* Refined at 2.0 Å Resolution. *Structure* 1994, 2 (11), 1073–1087. [PubMed: 7881907]
31. Cosgrove MS; Loh SN; Ha J-H; Levy HR, The Catalytic Mechanism of Glucose 6-Phosphate Dehydrogenases: Assignment and <sup>1</sup>H NMR Spectroscopy pH Titration of the Catalytic Histidine Residue in the 109 kDa *Leuconostoc mesenteroides* Enzyme. *Biochemistry* 2002, 41 (22), 6939–6945. [PubMed: 12033926]
32. Hamilton NM; Dawson M; Fairweather EE; Hamilton NS; Hitchin JR; James DI; Jones SD; Jordan AM; Lyons AJ; Small HF; Thomson GJ; Waddell ID; Ogilvie DJ, Novel Steroid Inhibitors of Glucose 6-Phosphate Dehydrogenase. *J. Med. Chem* 2012, 55 (9), 4431–4445. [PubMed: 22506561]
33. Freilich D; Ferris S; Wallace M; Leach L; Kallen A; Frincke J; Ahlem C; Hacker M; Nelson D; Hebert J, 16 $\alpha$ -Bromoepiandrosterone, a Dehydroepiandrosterone (DHEA) Analogue, Inhibits *Plasmodium falciparum* and *Plasmodium berghei* Growth. *Am. J. Trop. Med* 2000, 63 (5), 280–283.
34. Rasmussen KR; Arrowood MJ; Healey MC, Effectiveness of Dehydroepiandrosterone in Reduction of Cryptosporidial Activity in Immunosuppressed Rats. *Antimicrob. Agents Chemother* 1992, 36 (1), 220–222. [PubMed: 1534212]
35. Morales-Montor J; Baig S; Mitchell R; Deway K; Hallal-Calleros C; Damian RT, Immunoendocrine Interactions During Chronic Cysticercosis Determine Male Mouse Feminization: Role of IL-6. *J. Immunol* 2001, 167 (8), 4527–4533. [PubMed: 11591780]
36. dos Santos CD; Toldo MPA; Júnior J. C. d. P., Trypanosoma cruzi: The Effects of Dehydroepiandrosterone (DHEA) Treatment during Experimental Infection. *Acta Trop* 2005, 95 (2), 109–115. [PubMed: 15955522]
37. Vargas-Villavicencio JA; Larralde C; Morales-Montor J, Treatment with Dehydroepiandrosterone *in vivo* and *in vitro* Inhibits Reproduction, Growth and Viability of *Taenia crassiceps* metacystodes. *Int. J. Parasitol* 2008, 38 (7), 775–781. [PubMed: 18082750]
38. Carrero JC; Cervantes C; Moreno-Mendoza N; Saavedra E; Morales-Montor J; Laclette JP, Dehydroepiandrosterone Decreases while Cortisol Increases *in vitro* Growth and Viability of *Entamoeba histolytica*. *Microb. Infect* 2006, 8 (2), 323–331.
39. Cordeiro AT; Thiemann OH; Michels PAM, Inhibition of *Trypanosoma brucei* Glucose-6-phosphate Dehydrogenase by Human Steroids and their Effects on the Viability of Cultured Parasites. *Bioorg. Med. Chem* 2009, 17 (6), 2483–2489. [PubMed: 19231202]
40. Cordeiro AT; Thiemann OH, 16-Bromoepiandrosterone, an Activator of the Mammalian Immune System, Inhibits Glucose 6-phosphate Dehydrogenase from *Trypanosoma Cruzi* and Is Toxic to These Parasites Grown in Culture. *Bioorg. Med. Chem* 2010, 18 (13), 4762–4768. [PubMed: 20570159]
41. Fredo Naciuk F; do Nascimento Faria J; Gonçalves Eufrásio A; Torres Cordeiro A; Bruder M, Development of Selective Steroid Inhibitors for the Glucose-6-phosphate Dehydrogenase from *Trypanosoma cruzi*. *ACS Med. Chem. Lett* 2020, 11 (6), 1250–1256. [PubMed: 32551008]
42. Eberling P; Koivisto VA, Physiological Importance of Dehydroepiandrosterone. *Lancet* 1994, 343 (8911), 1479–1481. [PubMed: 7911183]
43. O'Shaughnessy PJ; Antignac JP; Le Bizet B; Morvan M-L; Svechnikov K; Söder O; Savchuk I; Monteiro A; Soffientini U; Johnston ZC; Bellingham M; Hough D; Walker N; Filis P; Fowler PA, Alternative (backdoor) Androgen Production and Masculinization in the Human Fetus. *PLoS Biol* 2019, 17 (2), e3000002. [PubMed: 30763313]
44. Mercaldi GF; Ranzani AT; Cordeiro AT, Discovery of New Uncompetitive Inhibitors of Glucose-6-Phosphate Dehydrogenase. *J. Biomol. Screen* 2014, 19 (10), 1362–1371. [PubMed: 25121555]
45. Martinez-Irujo JJ; Villahermosa ML; Mercapide J; Cabodevilla JF; Santiago E, Analysis of the Combined Effect of Two Linear Inhibitors on a Single Enzyme. *Biochem. J* 1998, 329 (3), 689–698. [PubMed: 9445400]
46. Theorell H; Yonetani T, Studies on Liver Alcohol Dehydrogenase Complexes: IV. Spectrophotometric Observations on the Enzyme Complexes. *Arch. Biochem. Biophys* 1964, 106, 252–258. [PubMed: 14217166]

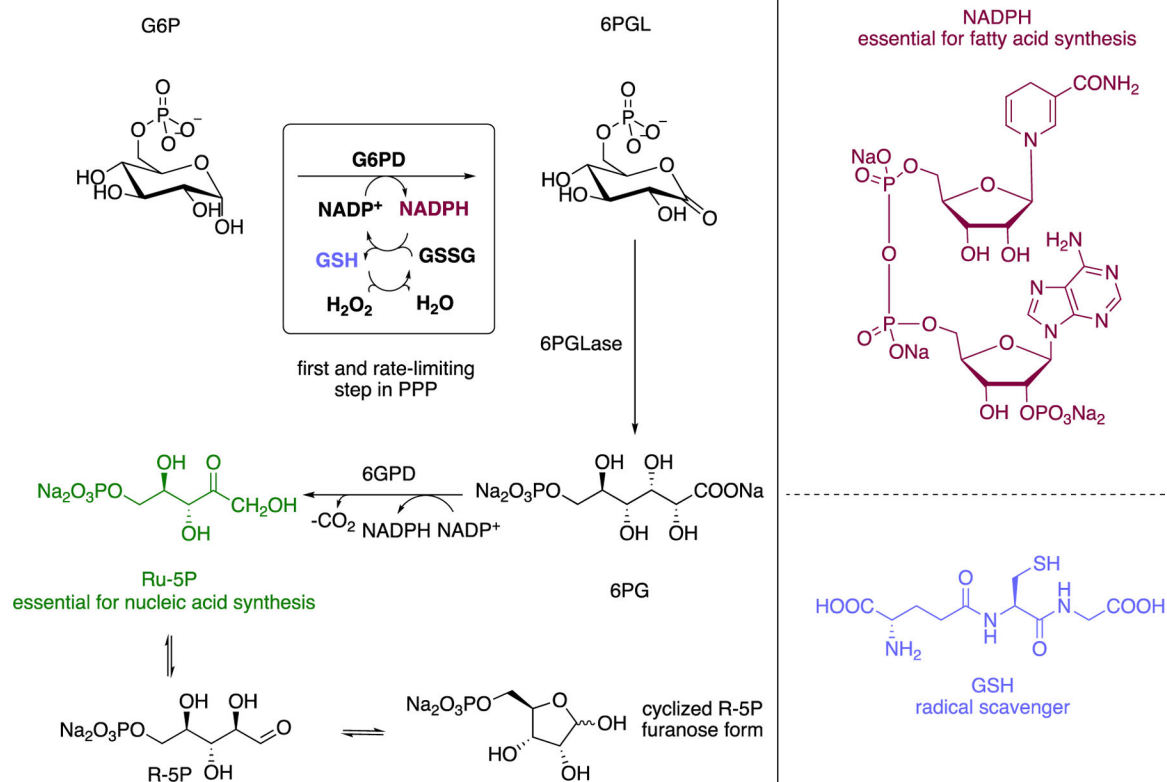
47. O'Brien E; Kurdi-Haidar B; Wanachiwanawin W; Carvajal J-L; Vulliamy TJ; Cappadoro M; Mason PJ; Luzzatto L, Cloning of the Glucose 6-phosphate Dehydrogenase Gene from *Plasmodium falciparum*. *Mol. Biochem. Parasitol* 1994, 64 (2), 313–326. [PubMed: 7935609]
48. Clarke JL; Scopes DA; Sodeinde O; Mason PJ, Glucose-6-phosphate Dehydrogenase-6-phosphogluconolactonase. A Novel Bifunctional Enzyme in Malaria Parasites. *Eur. J. Biochem* 2001, 268 (7), 2013–2019. [PubMed: 11277923]
49. Scopes DA; Bautista JM; Vulliamy TJ; Mason PJ, *Plasmodium falciparum* Glucose-6-phosphate Dehydrogenase (G6PD) — the N-terminal Portion is Homologous to a Predicted Protein Encoded near to G6PD in *Haemophilus influenzae*. *Mol. Microbiol* 1997, 23 (4), 847–848. [PubMed: 9157254]
50. Clarke JL; Sodeinde O; Mason PJ, A Unique Insertion in *Plasmodium berghei* Glucose-6-phosphate Dehydrogenase-6-phosphogluconolactonase: Evolutionary and Functional Studies. *Mol. Biochem. Parasitol* 2003, 127 (1), 1–8. [PubMed: 12615331]
51. Preuss J; Hedrick M; Sergienko E; Pinkerton A; Mangravita-Novo A; Smith L; Marx C; Fischer E; Jortzik E; Rahlfs S; Becker K; Bode L, High-Throughput Screening for Small-Molecule Inhibitors of *Plasmodium falciparum* Glucose-6-Phosphate Dehydrogenase 6-Phosphogluconolactonase. *J. Biomol. Screen* 2012, 17 (6), 738–751. [PubMed: 22496096]
52. Shafiq N; Arshad U; Zarren G; Parveen S; Javed I; Ashraf A, A Comprehensive Review: Bio-Potential of Barbituric Acid and its Analogues. *Curr. Org. Chem* 2020, 24 (2), 129–161.
53. Meister A, Glutathione Metabolism and its Selective Modification. *J. Biol. Chem* 1988, 263 (33), 17205–17208. [PubMed: 3053703]
54. Forman HJ; Zhang H; Rinna A, Glutathione: Overview of its Protective Roles, Measurement, and Biosynthesis. *Mol. Asp. Med* 2009, 30 (1–2), 1–12.
55. Lauterburg BH; Corcoran GB; Mitchell JR, Mechanism of Action of N-acetylcysteine in the Protection against the Hepatotoxicity of Acetaminophen in Rats in Vivo. *J. Clin. Invest* 1983, 71 (4), 980–991. [PubMed: 6833497]
56. Guiguemde WA; Shelat AA; Bouck D; Duffy S; Crowther GJ; Davis PH; Smithson DC; Connelly M; Clark J; Zhu F; Jiménez-Díaz MB; Martínez MS; Wilson EB; Tripathi AK; Gut J; Sharlow ER; Bathurst I; El Mazouni F; Fowble JW; Forquer I; McGinley PL; Castro S; Angulo-Barturen I; Ferrer S; Rosenthal PJ; Derisi JL; Sullivan DJ; Lazo JS; Roos DS; Riscoe MK; Phillips MA; Rathod PK; Van Voorhis WC; Avery VM; Guy RK, Chemical Genetics of *Plasmodium falciparum*. *Nature* 2010, 465 (7296), 311–315. [PubMed: 20485428]
57. Jortzik E; Mailu Boniface M.; Preuss J; Fischer M; Bode L; Rahlfs S; Becker K, Glucose-6-phosphate Dehydrogenase–6-phosphogluconolactonase: A Unique Bifunctional Enzyme from *Plasmodium falciparum*. *Biochem. J* 2011, 436 (3), 641–650. [PubMed: 21443518]
58. Rana P; Naven R; Narayanan A; Will Y; Jones LH, Chemical Motifs that Redox Cycle and their Associated Toxicity. *MedChemComm* 2013, 4 (8), 1175–1180.
59. Johnston PA, Redox Cycling Compounds Generate H<sub>2</sub>O<sub>2</sub> in HTS buffers Containing Strong Reducing Reagents--Real Hits or Promiscuous Artifacts? *Curr. Opin. Chem. Biol* 2011, 15 (1), 174–182. [PubMed: 21075044]
60. Lor LA; Schneck J; McNulty DE; Diaz E; Brandt M; Thrall SH; Schwartz B, A Simple Assay for Detection of Small-molecule Redox Activity. *J Biomol. Screen* 2007, 12 (6), 881–890. [PubMed: 17579124]
61. Preuss J; Maloney P; Peddibhotla S; Hedrick MP; Hershberger P; Gosalia P; Milewski M; Li YL; Sugarman E; Hood B; Suyama E; Nguyen K; Vasile S; Sergienko E; Mangravita-Novo A; Vicchiarelli M; McAnally D; Smith LH; Roth GP; Diwan J; Chung TDY; Jortzik E; Rahlfs S; Becker K; Pinkerton AB; Bode L, Discovery of a *Plasmodium falciparum* Glucose-6-phosphate Dehydrogenase 6-phosphogluconolactonase Inhibitor (R,Z)-N-((1-Ethylpyrrolidin-2-yl)methyl)-2-(2-fluorobenzylidene)-3-oxo-3,4-dihydro-2H-benzo[b][1,4]thiazine-6-carboxamide (ML276) That Reduces Parasite Growth in Vitro. *J. Med. Chem* 2012, 55 (16), 7262–7272. [PubMed: 22813531]
62. Kaminsky D; Kryshchshyn A; Lesyk R, Recent Developments with Rhodanine as a Scaffold for Drug Discovery. *Expert Opin. Drug. Discov* 2017, 12 (12), 1233–1252. [PubMed: 29019278]



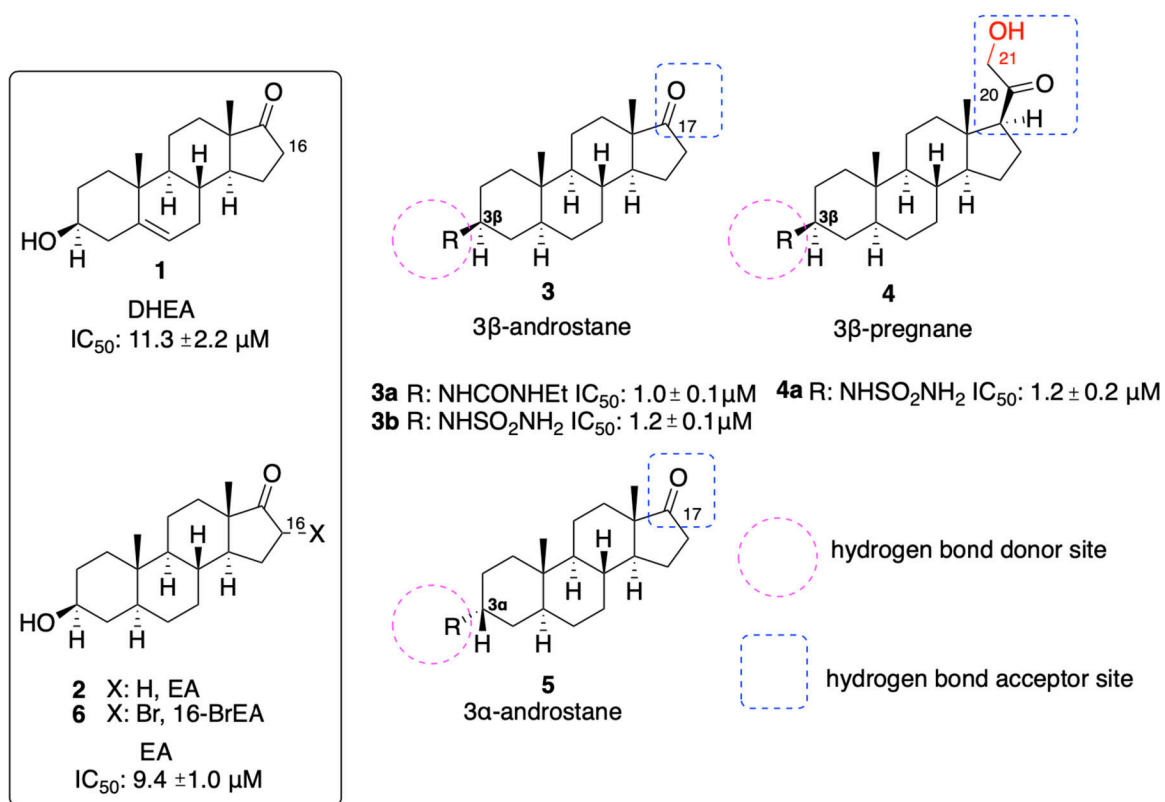
63. Sutanto F; Konstantinidou M; Dömling A, Covalent Inhibitors: A Rational Approach to Drug Discovery. *RSC Med. Chem* 2020, 11 (8), 876–884. [PubMed: 33479682]
64. Alencar N; Sola I; Linares M; Juárez-Jiménez J; Pont C; Viayna A; Vílchez D; Sampedro C; Abad P; Pérez-Benavente S; Lameira J; Bautista JM; Muñoz-Torrero D; Luque FJ, First Homology Model of Plasmodium falciparum Glucose-6-phosphate dehydrogenase: Discovery of Selective Substrate Analog-based Inhibitors as Novel Antimalarial Agents. *Eur. J. Med. Chem* 2018, 146, 108–122. [PubMed: 29407943]
65. Lu SC, Glutathione Synthesis. *Biochim. Biophys. Acta Gen. Subj* 2013, 1830 (5), 3143–3153.
66. Alkarakooly Z; Kilaparty S; Al-Anbaky Q; Khan M; Ali N, Dichloroacetic Acid (DCA)-Induced Cytotoxicity in Human Breast Cancer Cells Accompanies Changes in Mitochondrial Membrane Permeability and Production of Reactive Oxygen Species. *J. Canc. Ther* 2014, 5, 1234–1248.
67. Viayna A; Vílchez D; Vázquez J; Pérez-Benavente S; Bautista JM; Luque FJ, Searching for Selective Scaffolds against Plasmodium falciparum Glucose-6-Phosphate Dehydrogenase 6-Phosphogluconolactonase. *Proc* 2019, 22 (1), 28.
68. Haeussler K; Berneburg I; Jortzik E; Hahn J; Rahbari M; Schulz N; Preuss J; Zapol'skii VA; Bode L; Pinkerton AB; Kaufmann DE; Rahlfs S; Becker K, Glucose 6-phosphate Dehydrogenase 6-Phosphogluconolactonase: Characterization of the Plasmodium vivax Enzyme and Inhibitor Studies. *Malar. J* 2019, 18 (1), 22–22. [PubMed: 30683097]
69. Erlanson DA; Braisted AC; Raphael DR; Randal M; Stroud RM; Gordon EM; Wells JA, Site-Directed Ligand Discovery. *Proc. Natl. Acad. Sci* 2000, 97 (17), 9367–9372. [PubMed: 10944209]
70. Maloney P; Hedrick M; Peddibhotla S; Hershberger P; Milewski M; Gosalia P; Li L; Preuss J; Sugarman E; Hood B; Suyama E; Nguyen K; Vasile S; Sergienko E; Salanawil S; Stonich D; Su Y; Dahl R; Mangravita-Novo A; Vicchiarelli M; McAnally D; Smith LH; Roth G; Diwan J; Chung TDY; Pinkerton AB; Bode L; Becker K, A 2nd Selective Inhibitor of Plasmodium falciparum Glucose-6-Phosphate Dehydrogenase (PfG6PDH) - Probe 2. In *Probe Reports from the NIH Molecular Libraries Program*, National Center for Biotechnology Information (US): Bethesda (MD), 2010.
71. Preuss J; Richardson AD; Pinkerton A; Hedrick M; Sergienko E; Rahlfs S; Becker K; Bode L, Identification and Characterization of Novel Human Glucose-6-Phosphate Dehydrogenase Inhibitors. *J. Biomol. Screen* 2013, 18 (3), 286–297. [PubMed: 23023104]
72. Torchilin VP, Passive and Active Drug Targeting: Drug Delivery to Tumors as an Example. *Handb. Exp. Pharmacol* 2010, (197), 3–53.
73. Senesi S; Csala M; Marcolongo P; Fulceri R; Mandl J; Banhegyi G; Benedetti A, Hexose-6-phosphate Dehydrogenase in the Endoplasmic Reticulum. *Biol. Chem* 2010, 391 (1), 1–8. [PubMed: 19804362]
74. Hewitt KN; Walker EA; Stewart PM, Minireview: Hexose-6-phosphate dehydrogenase and Redox control of 11 $\beta$ -Hydroxysteroid Dehydrogenase Type 1 Activity. *Endocrinology* 2005, 146 (6), 2539–43. [PubMed: 15774558]
75. Mason PJ; Stevens D; Diez A; Knight SW; Scopes DA; Vulliamy TJ, Human Hexose-6-phosphate Dehydrogenase (Glucose 1-Dehydrogenase) Encoded at 1p36: Coding Sequence and Expression. *Blood Cells Mol. Dis* 1999, 25 (1), 30–7. [PubMed: 10349511]
76. Beutler E; Morrison M, Localization and Characteristics of Hexose 6-Phosphate Dehydrogenase (Glucose Dehydrogenase). *J. Biol. Chem* 1967, 242 (22), 5289–93. [PubMed: 4169027]
77. Cossu V; Bonanomi M; Bauckneht M; Ravera S; Righi N; Miceli A; Morbelli S; Orenco AM; Piccioli P; Bruno S; Gaglio D; Sambuceti G; Marini C, Two High-rate Pentose-phosphate Pathways in Cancer Cells. *Sci. Rep* 2020, 10 (1), 22111. [PubMed: 33335166]
78. Ghergurovich JM; García-Cañaveras JC; Wang J; Schmidt E; Zhang Z; TeSlaa T; Patel H; Chen L; Britt EC; Piqueras-Nebot M; Gomez-Cabrera MC; Lahoz A; Fan J; Beier UH; Kim H; Rabinowitz JD, A Small Molecule G6PD Inhibitor Reveals Immune Dependence on Pentose Phosphate Pathway. *Nat. Chem. Biol* 2020, 16, 731–739. [PubMed: 32393898]
79. Zamani S; Hoseini AZ; Namin AM, Glucose-6-phosphate Dehydrogenase (G6PD) Activity Can Modulate Macrophage Response to Leishmania Major Infection. *Int. Immunopharmacol* 2019, 69, 178–183. [PubMed: 30716588]

80. Tu D; Gao Y; Yang R; Guan T; Hong JS; Gao HM, The Pentose Phosphate Pathway Regulates Chronic Neuroinflammation and Dopaminergic Neurodegeneration. *J. Neuroinflammation* 2019, 16 (1), 255. [PubMed: 31805953]
81. Park YJ; Choe SS; Sohn JH; Kim JB, The Role of Glucose-6-phosphate Dehydrogenase in Adipose Tissue Inflammation in Obesity. *Adipocyte* 2017, 6 (2), 147–153. [PubMed: 28425844]
82. Abdullaha M; Mohammed S; Ali M; Kumar A; Vishwakarma RA; Bharate SB, Discovery of Quinazolin-4(3H)-ones as NLRP3 Inflammasome Inhibitors: Computational Design, Metal-free Synthesis, and in vitro Biological Evaluation. *J. Org. Chem* 2019, 84 (9), 5129–5140. [PubMed: 30896160]
83. Zahid A; Li B; Kombe AJK; Jin T; Tao J, Pharmacological Inhibitors of the NLRP3 Inflammasome. *Front. Immunol* 2019, 10, 2538. [PubMed: 31749805]
84. Hour M-J; Huang L-J; Kuo S-C; Xia Y; Bastow K; Nakanishi Y; Hamel E; Lee K-H, 6-Alkylamino- and 2,3-Dihydro-3'-methoxy-2-phenyl-4-quinazolinones and Related Compounds: Their Synthesis, Cytotoxicity, and Inhibition of Tubulin Polymerization. *J. Med. Chem* 2000, 43 (23), 4479–4487. [PubMed: 11087572]
85. Ceramella J; Caruso A; Occhiuzzi MA; Iacopetta D; Barbarossa A; Rizzuti B; Dallemagne P; Rault S; El-Kashef H; Saturnino C; Grande F; Sinicropi MS, Benzothienoquinazolinones as New Multi-target Scaffolds: Dual Inhibition of Human Topoisomerase I and Tubulin Polymerization. *Eur. J. Med. Chem* 2019, 181, 111583. [PubMed: 31400710]
86. Hejazi L; Rezaee E; Tabatabai SA, Quinazoline-4(3H)-one Derivatives as Novel and Potent Inhibitors of Soluble Epoxide Hydrolase: Design, Synthesis and Biological Evaluation. *Bioorg. Chem* 2020, 99, 103736. [PubMed: 32229350]
87. Ramírez-Nava EJ; Hernández-Ochoa B; Navarrete-Vázquez G; Arreguín-Espinosa R; Ortega-Cuellar D; González-Valdez A; Martínez-Rosas V; Morales-Luna L; Martínez-Miranda J; Sierra-Palacios E; Rocha-Ramírez LM; De Franceschi L; Marcial-Quino J; Gómez-Manzo S, Novel Inhibitors of Human Glucose-6-phosphate Dehydrogenase (HsG6PD) Affect the Activity and Stability of the Protein. *Biochim. Biophys. Acta Gen. Subj* 2021, 1865 (3), 129828. [PubMed: 33347959]
88. Beno BR; Yeung K-S; Bartberger MD; Pennington LD; Meanwell NA, A Survey of the Role of Noncovalent Sulfur Interactions in Drug Design. *J. Med. Chem* 2015, 58 (11), 4383–4438. [PubMed: 25734370]
89. Ortiz C; Moraca F; Medeiros A; Botta M; Hamilton N; Comini MA, Binding Mode and Selectivity of Steroids towards Glucose-6-phosphate Dehydrogenase from the Pathogen *Trypanosoma cruzi*. *Molecules* 2016, 21 (3), 368. [PubMed: 26999093]
90. Ortíz C; Moraca F; Laverriere M; Jordan A; Hamilton N; Comini MA, Glucose 6-Phosphate Dehydrogenase from Trypanosomes: Selectivity for Steroids and Chemical Validation in Bloodstream *Trypanosoma brucei*. *Molecules* 2021, 26 (2), 358.
91. Dodds EC; Goldberg L; Lawson W; Robinson R, OEstrogenic Activity of Certain Synthetic Compounds. *Nature* 1938, 141 (3562), 247–248.
92. Jordan VC; Morrow M, Tamoxifen, Raloxifene, and the Prevention of Breast Cancer. *Endocr. Rev* 1999, 20 (3), 253–278. [PubMed: 10368771]
93. Bentrem DJ; Craig Jordan V, Tamoxifen, Raloxifene and the Prevention of Breast Cancer. *Minerva Endocrinol* 2002, 27 (2), 127–139. [PubMed: 11961504]
94. Nettles KW; Bruning JB; Gil G; O'Neill EE; Nowak J; Guo Y; Kim Y; DeSombre ER; Dilis R; Hanson RN; Joachimiak A; Greene GL, Structural plasticity in the Oestrogen Receptor Ligand-binding Domain. *EMBO Rep* 2007, 8 (6), 563–568. [PubMed: 17468738]
95. Shiau AK; Barstad D; Loria PM; Cheng L; Kushner PJ; Agard DA; Greene GL, The Structural Basis of Estrogen Receptor/Coactivator Recognition and the Antagonism of This Interaction by Tamoxifen. *Cell* 1998, 95 (7), 927–937. [PubMed: 9875847]
96. Sikder A; Chakraborty S; Rajdev P; Dey P; Ghosh S, Molecular Recognition Driven Bioinspired Directional Supramolecular Assembly of Amphiphilic (Macro)molecules and Proteins. *Acc. Chem. Res* 2021, 54 (11), 2670–2682. [PubMed: 34014638]
97. Singh J; Petter RC; Baillie TA; Whitty A, The Resurgence of Covalent Drugs. *Nat. Rev. Drug Discov* 2011, 10 (4), 307–317. [PubMed: 21455239]

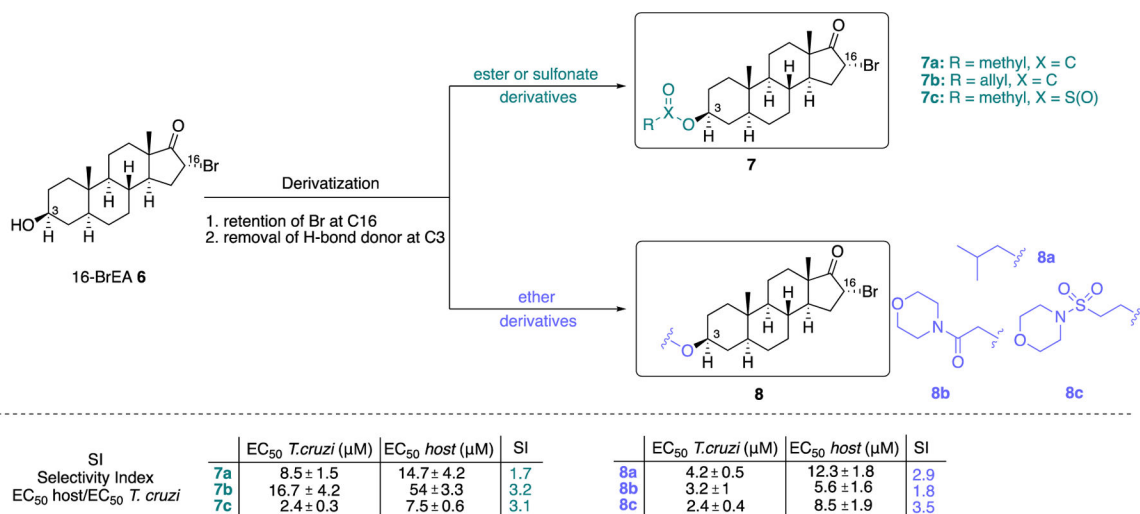
98. Bauer RA, Covalent Inhibitors in Drug Discovery: From Accidental Discoveries to Avoided Liabilities and Designed Therapies. *Drug Discov. Today* 2015, 20 (9), 1061–1073. [PubMed: 26002380]
99. Bian Y; Jun JJ; Cuyler J; Xie X-Q, Covalent Allosteric Modulation: An Emerging Strategy for GPCRs Drug Discovery. *Eur. J. Med. Chem* 2020, 206, 112690. [PubMed: 32818870]
100. Ostrem JM; Peters U; Sos ML; Wells JA; Shokat KM, K-Ras(G12C) Inhibitors Allosterically Control GTP Affinity and Effector Interactions. *Nature* 2013, 503 (7477), 548–551. [PubMed: 24256730]
101. Ostrem JML; Shokat KM, Direct Small-molecule Inhibitors of KRAS: From Structural Insights to Mechanism-based Design. *Nat. Rev. Drug Discov* 2016, 15 (11), 771–785. [PubMed: 27469033]
102. Erlanson DA; Davis B; Jahnke W, Fragment-Based Drug Discovery: Advancing Fragments in the Absence of Crystal Structures. *Cell Chem. Biol* 2019, 26 1, 9–15. [PubMed: 30482678]
103. Erlanson DA; Wells JA; Braisted AC, Tethering: Fragment-based Drug Discovery. *Annu. Rev. Biophys. Biomol. Struct* 2004, 33, 199–223. [PubMed: 15139811]
104. Köhler E; Barrach H; Neubert D, Inhibition of NADP<sup>+</sup> Dependent Oxidoreductases by the 6-Aminonicotinamide Analogue of NADP<sup>+</sup>. *FEBS Lett* 1970, 6 (3), 225–228. [PubMed: 11947380]

**Figure 1.**

The Pentose Phosphate Pathway (PPP); implication in redox homeostasis and cell proliferation.

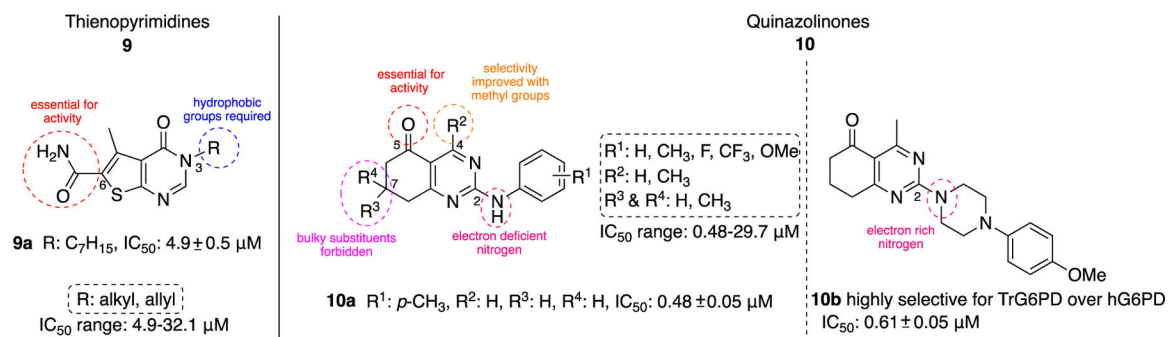


**Figure 2.**  
DHEA **1**, EA **2**, and newer steroidal analogues as inhibitors of hG6PD and TrG6PD.

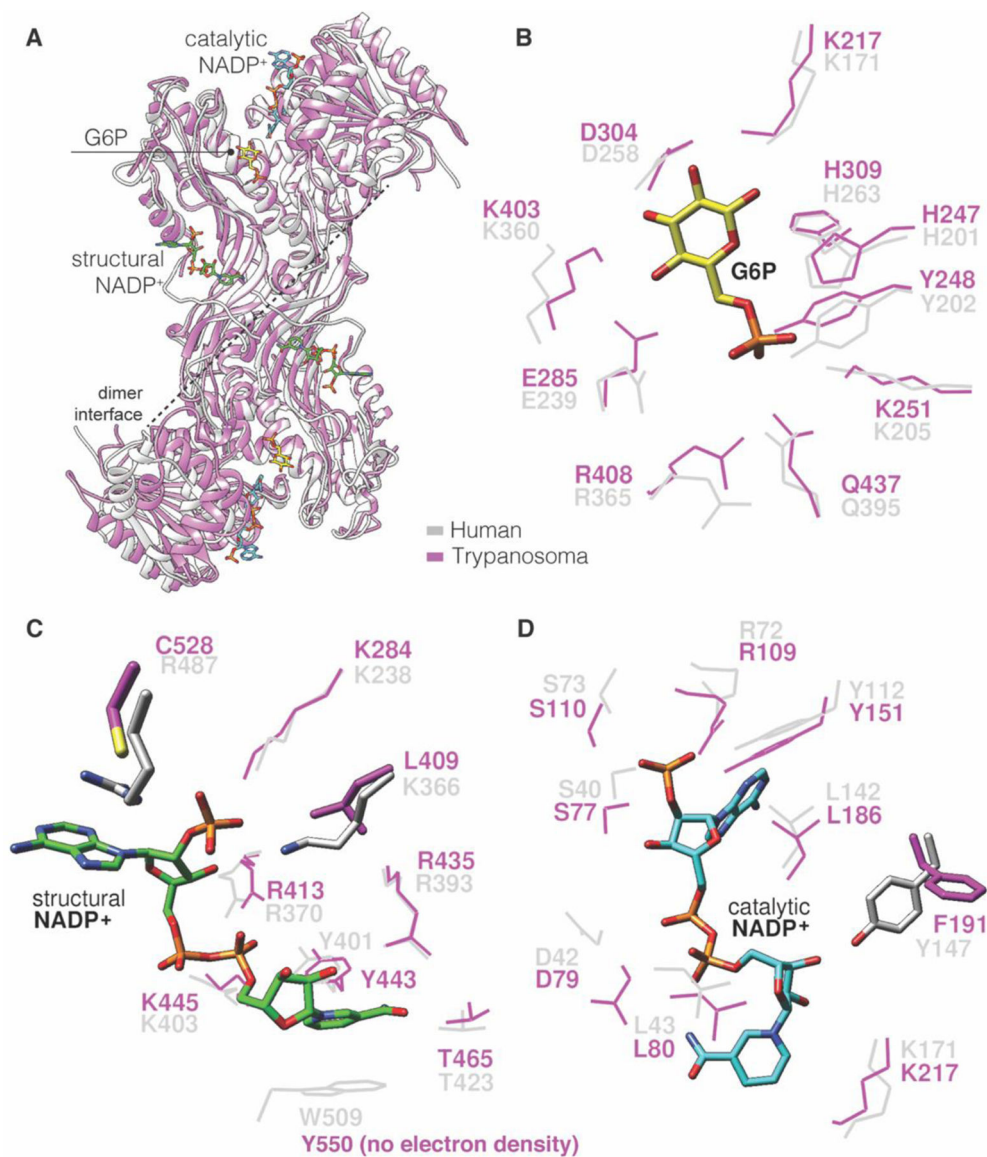


**Figure 3.**  
Derivatives of **6** as selective (**7a-7b**, selective for TrG6PD over hG6PD) and potent (**7c**, **8a-c**) steroidal inhibitors.

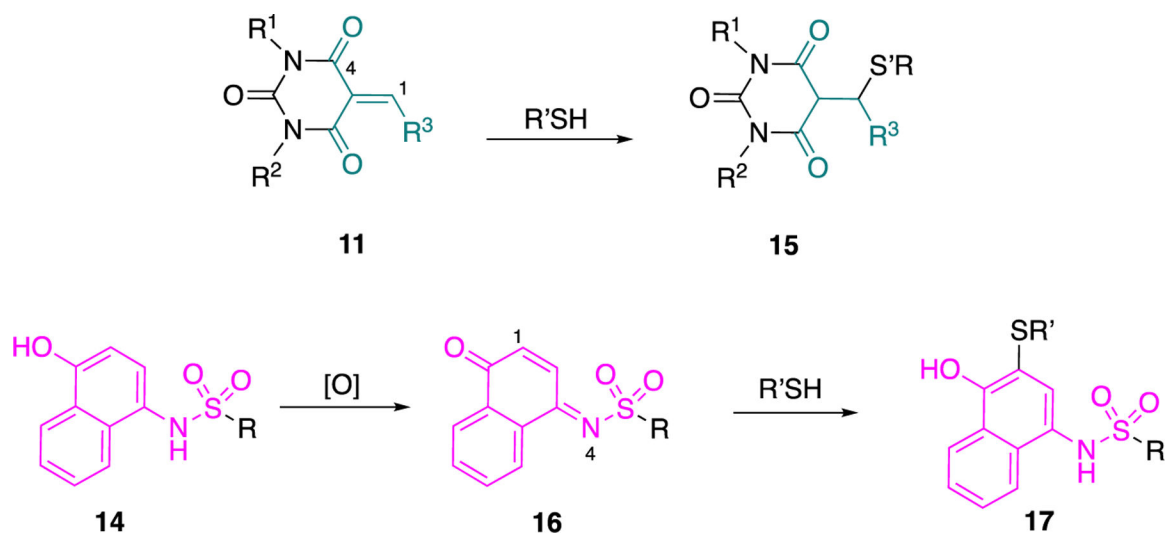




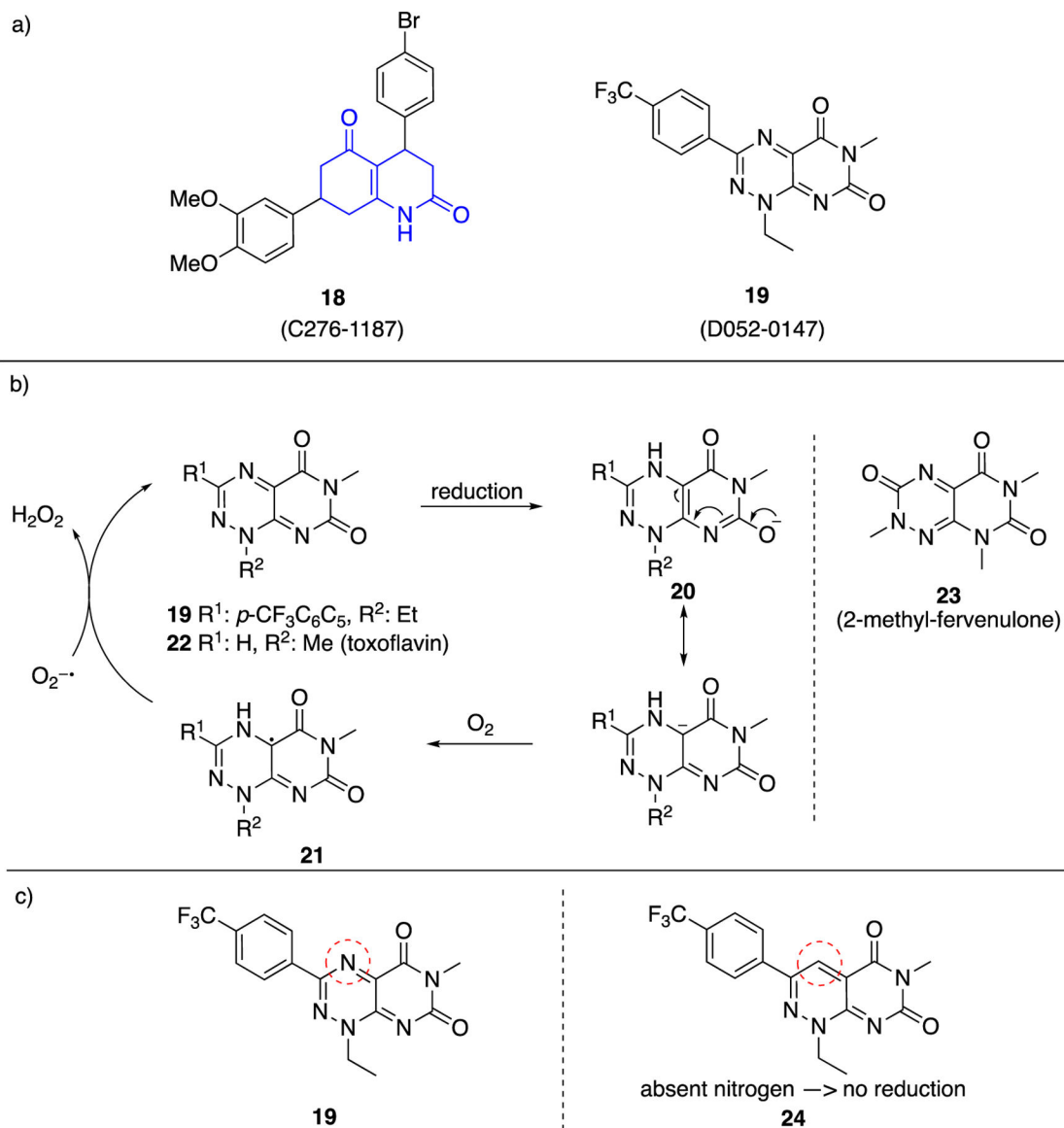
**Figure 4.** Thienopyrimidine- and quinazoline-containing compounds of type **9** and **10**: potent against recombinant TrG6PD; IC<sub>50</sub> values and ranges come from measurements against recombinant TrG6PD.



**Figure 5.**  
A. Overlay hG6PD (PDB ID: 2BH9) and TrG6PD (PDB ID: 5AQ1), grey for hG6PD and purple for TrG6PD; B. Overlay of the catalytic G6P site hG6PD-TrG6PD; C. Overlay of the structural NADP<sup>+</sup> in hG6PD with respective region in TrG6PD lacking the structural NADP<sup>+</sup>. D. Overlay of the catalytic NADP<sup>+</sup> site hG6PD-TrG6PD.



**Figure 6.**  
Compounds of type **11** and **14** as promiscuous substrates for Michael addition.

**Figure 7.**

a. Commercially available **18** (C276–1187) and **19** (D052–0147) shown to inhibit *P.falciparum*; b. Pyrimidine triazinodiones **19**, **22**, **23** lead to radical intermediates **21** and H<sub>2</sub>O<sub>2</sub> release; c. Strategy of replacing triazine with pyridazine to prevent first reduction step shown in 7b.

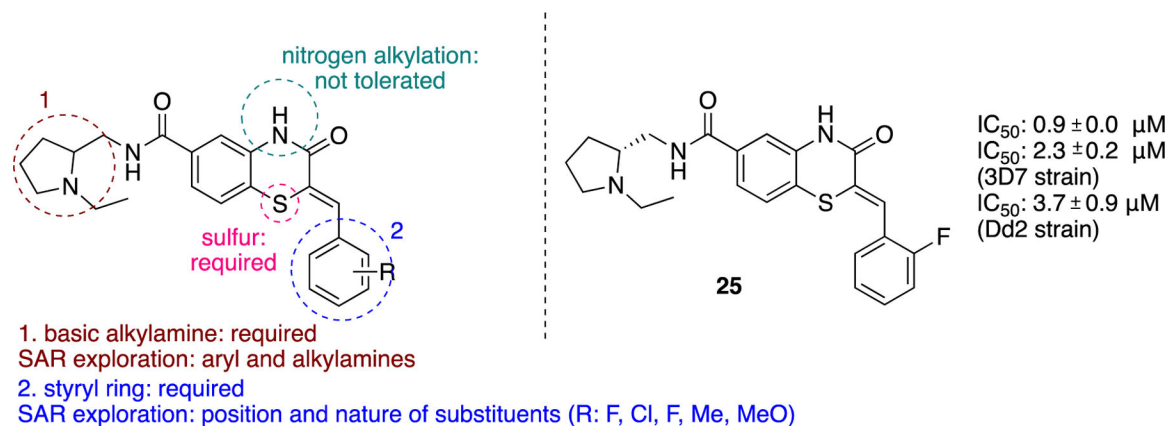
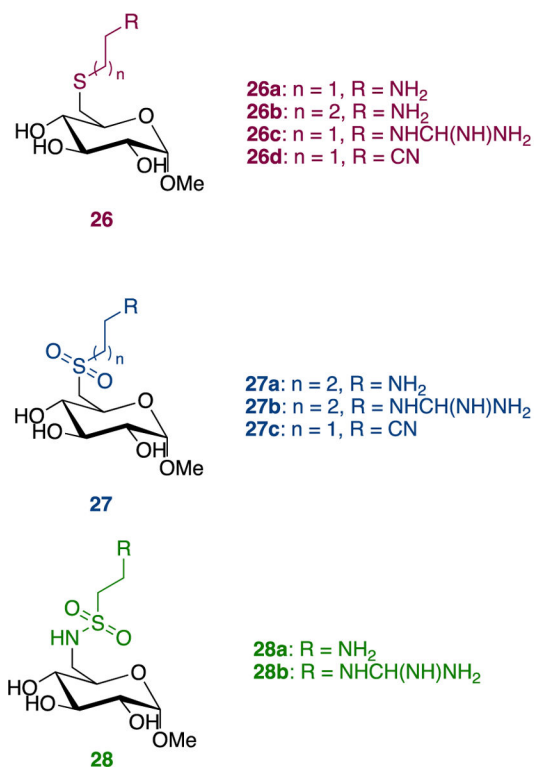
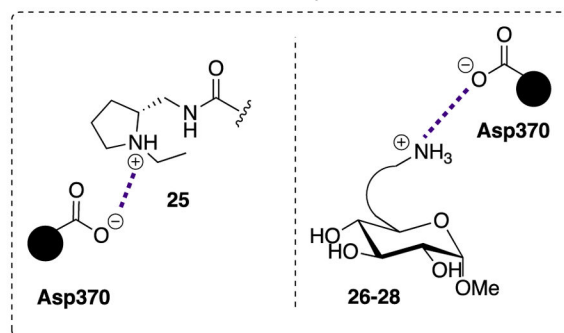


**Figure 8.**  
Generic benzothiazinone ring, essential features for activity, SAR exploration and specific PfGluPho compound **25**.



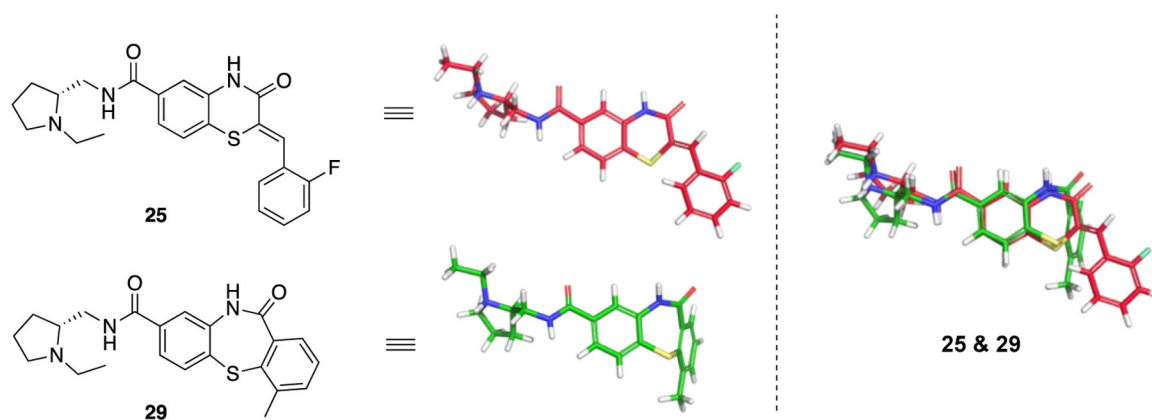
	$K_i$ PfGluPho ( $\mu\text{M}$ )	$K_i$ hG6PD ( $\mu\text{M}$ )	SI
<b>26a</b>	<b>76.1</b>	<b>&gt;2000</b>	<b>&gt;26</b>
<b>26b</b>	289	129	0.4
<b>26c</b>	45.6	>200	>4.4
<b>26d</b>	259	>200	>0.8
<b>27a</b>	34.4	35.4	1.0
<b>27b</b>	42.9	22.3	0.5
<b>27c</b>	68.8	>200	>2.9
<b>28a</b>	<b>22.8</b>	<b>&gt;400</b>	<b>&gt;18</b>
<b>28b</b>	32.4	16.8	0.5

Predicted ionic interaction of non-glucosidic analog **25** and glucosidic analogs **26-28** with Asp370



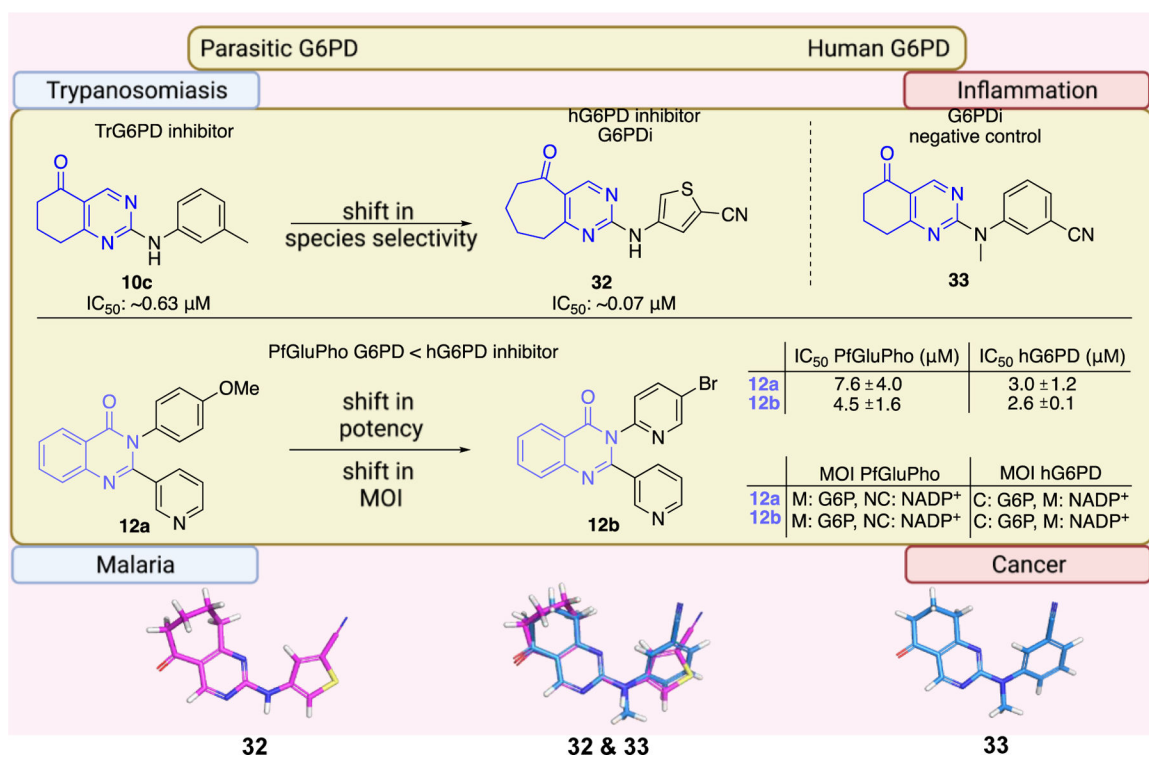
**Figure 9.** Compounds **26–28**, *in vitro* biochemical activity  $K_i$  for G6P, and proposed interactions of non-glucosidic compound **25** and glucosidic compounds **26–28** with Asp370.



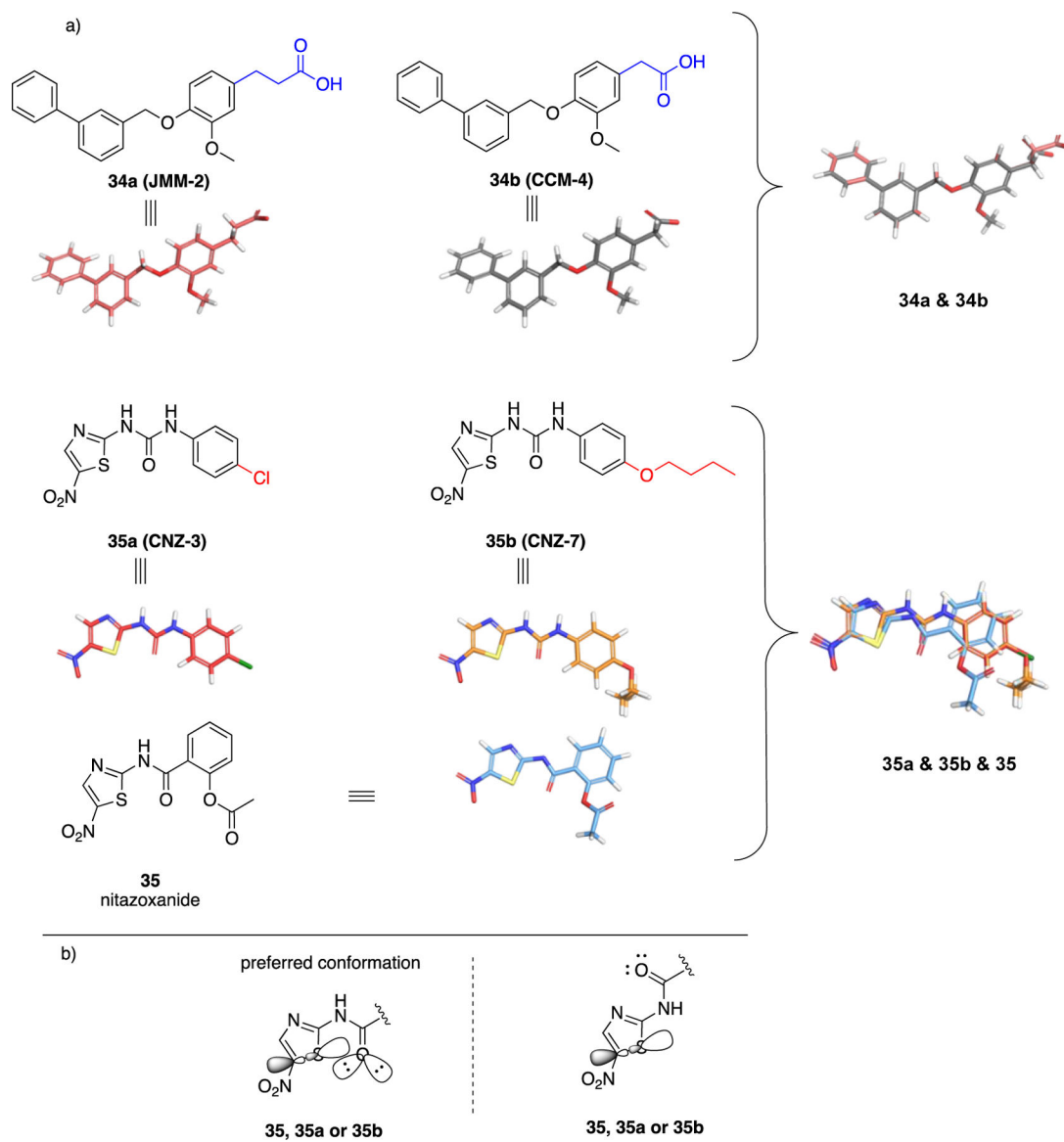


**Figure 10.**

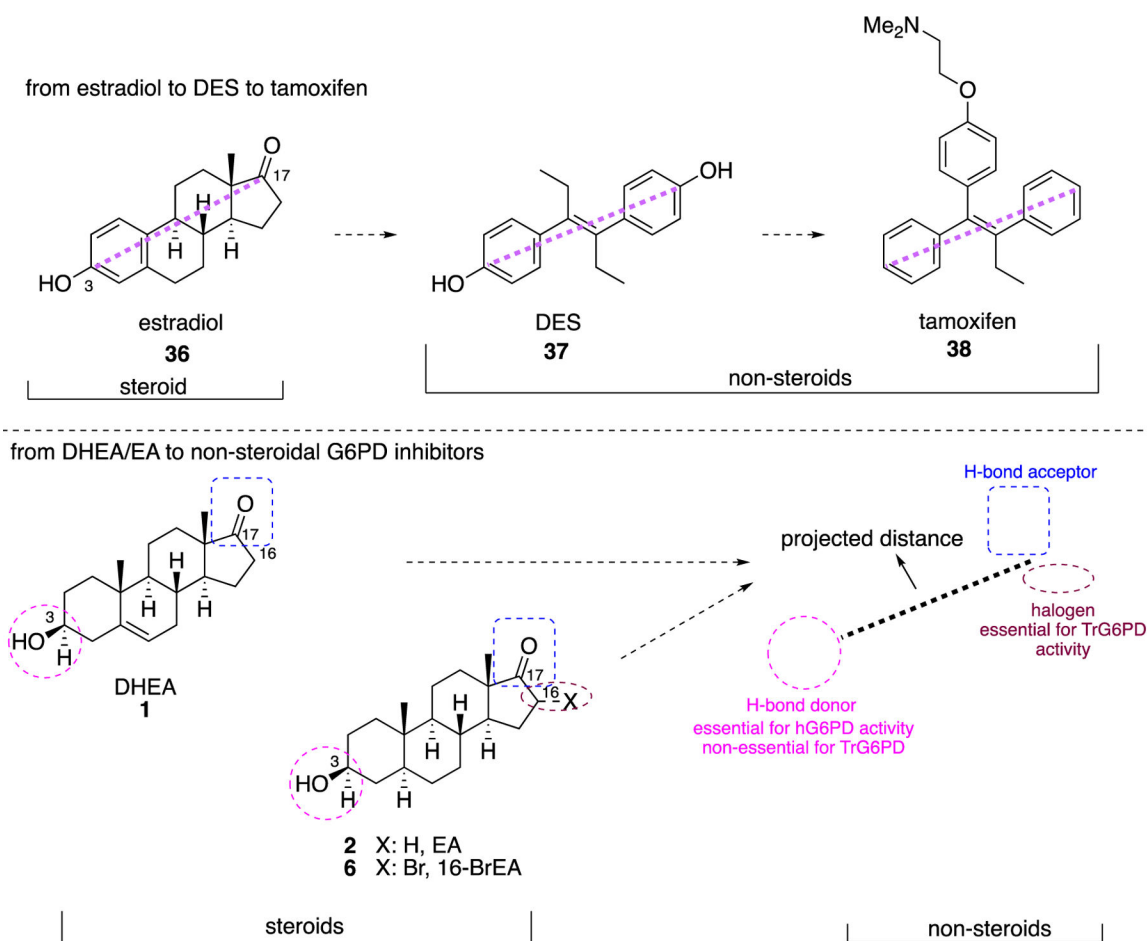
Compounds **25** (ML276) and compound **29** (ML304). 3D alignment performed with Schrödinger 2021–3, Maestro, using largest Bemis-Murcko scaffold. ML276 and ML304 as taken from the original paper.

**Figure 11.**

Generic structures of non-steroidal G6PD inhibitors used in infectious diseases, inflammation, and cancer. Main core observed in all cases: quinazolinone. Ligand alignment performed with Schrödinger 2021–3, Maestro, using largest Bemis-Murcko scaffold. M: mixed-type, NC: non-competitive, C: competitive, MOI: modality of inhibition. [Biorender.com](https://www.biorender.com) was used in part for Figure 11.

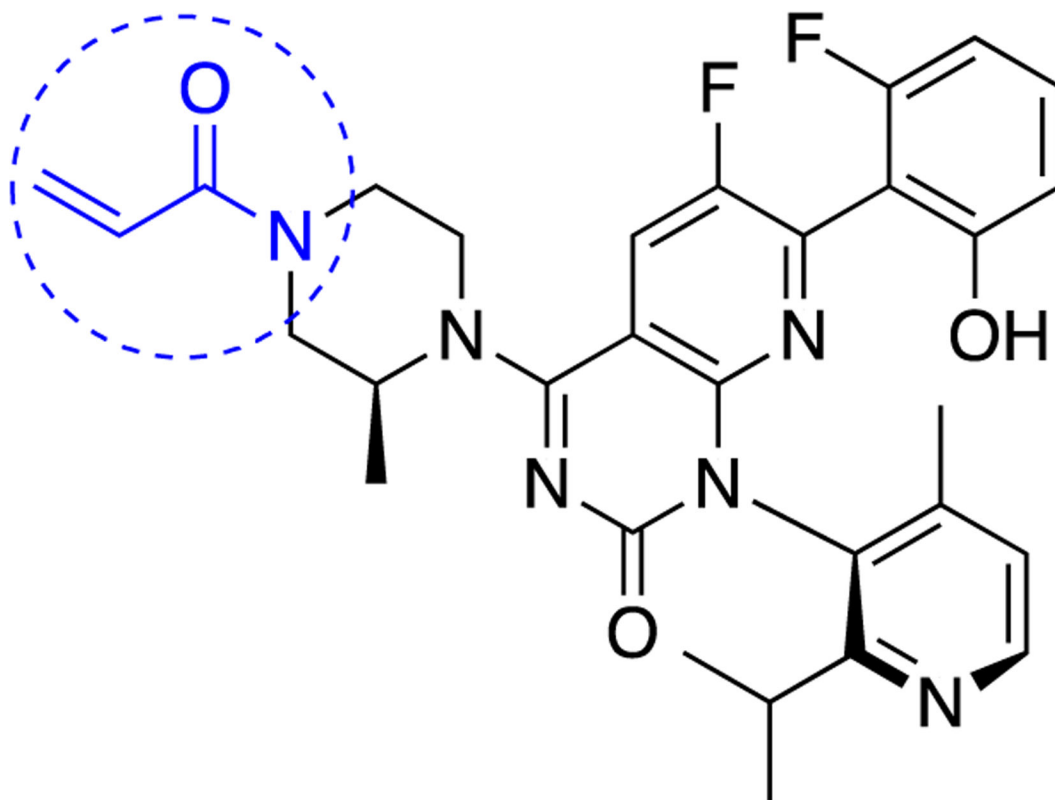
**Figure 12.**

a. Compounds **34a**, **34**, **35a**, **35b** showed inhibitory activity against hG6PD and used for blind molecular docking; Codes in parenthesis as taken from the original paper. Ligand alignment performed with Schrödinger 2021–3, Maestro, using largest Bemis-Murcko scaffold for **34a** & **34b** and sample reference **35a** for **35a**, **35b** & **35**; b. Preferred conformation of the nitro compounds **35**, **35a** & **35b**: overlap of the non-bonding lone pair of oxygen with the  $\sigma^*$  orbital of sulfur.

**Figure 13.**

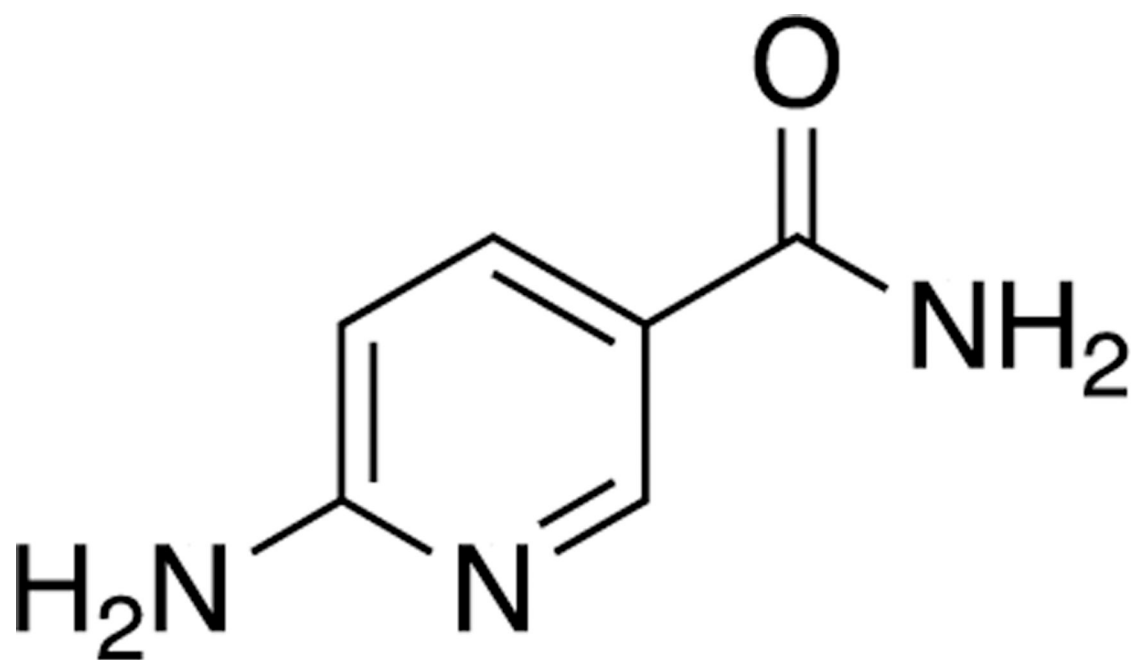
Top: from estradiol (**36**) to DES (**37**) to tamoxifen (**38**); bottom; perspective for transition of steroidal **1**, **2**, **6** to non-steroidal analogues.

reactive and discriminate  
Michael acceptor



## AMG510 39

**Figure 14.** AMG510 **39**, selective KRAS inhibitor for cancerous cells; designed for molecular recognition and for specific reaction with Cys12 in mutated malignant cells.



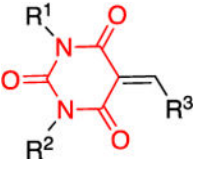
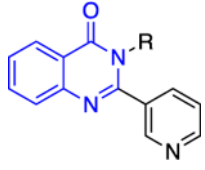
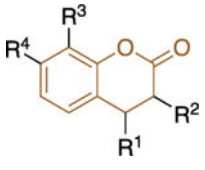
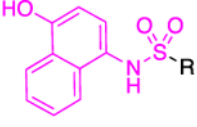
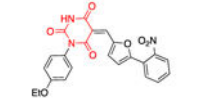
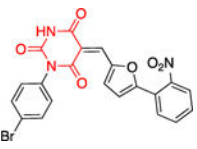
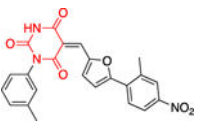
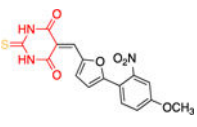
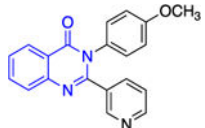
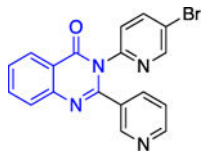
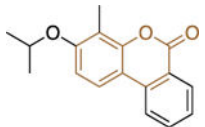
# 6-aminonicotinamide 40

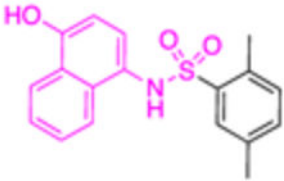
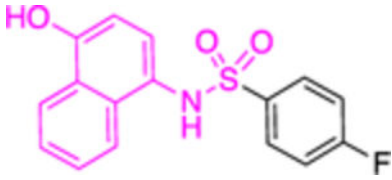
**Figure 15.**  
6-Aminonicotinamide **40**, a potential fragment for FBDD of competitive G6PD inhibitors.



Table 1.

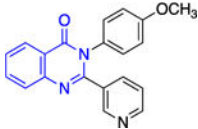
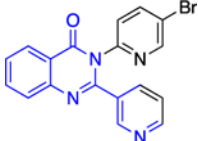
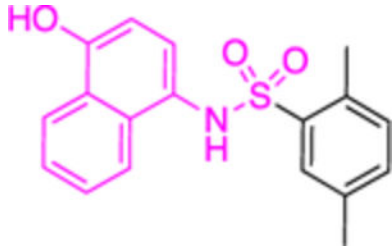
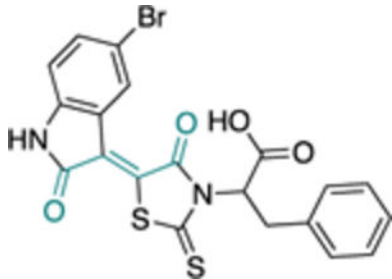
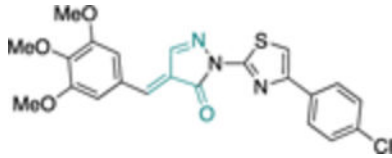
Structural classification of PfGluPho inhibitors identified by the Bode group; Numbers in parenthesis (as taken from the original paper).

Compounds	Class 1 pyrimidinones 11	Class 2 quinazolinones 12	Class 3 chromenones 13	Class 4 sulfonamides 14	PfGluPho IC <sub>50</sub> ( $\mu$ M) recomb.	PfGluPho IC <sub>50</sub> ( $\mu$ M) cult.
						
11a (CB64)					19.9 ± 7.2	-
11b (CB62)					11.6 ± 1.0	-
11c (CB61)					5.1 ± 3.2	-
11d (CB22)					4.6 ± 2.4	-
12a (CB104)					7.6 ± 4.0	-
12b (CB70)					4.5 ± 1.6	-
13a (CB103)					1.5 ± 0.4	0.97 ± 0.15

Compounds	Class 1 pyrimidinones 11	Class 2 quinazolinones 12	Class 3 chromenones 13	Class 4 sulfonamides 14	PfGluPho IC <sub>50</sub> ( $\mu$ M) recomb.	PfGluPho IC <sub>50</sub> ( $\mu$ M) cult.
14a (CB83)					22.0 $\pm$ 8.0	5.3 $\pm$ 2
14b (CB90)					>30	3.9 $\pm$ 0.14

**Table 2.**

Comparison of IC<sub>50</sub> values for PfGluPho and hG6PD; shift of focus from antimalarial to anticancer agents by the Bode group; Numbers in parenthesis as taken from the original paper. For **14a** 1: (w/ pre-incubation and post-dilution), 2: (only pre-incubation).

Compound	Structure	PfGluPho IC <sub>50</sub> (μM)	IC <sub>50</sub> Comparison	hG6PD IC <sub>50</sub> (μM)
12a (CB104)		7.6 ± 4.0	>	3.0 ± 1.2
12b (CB70)		4.5 ± 1.6	>	2.6 ± 0.1
14a (CB83)		22.0 ± 0.8	>	0.2 ± 0.0 <sup>1</sup> or 0.4 ± 0.0 <sup>2</sup>
30 (CB72)		-		3.1 ± 0.8
31 (CB63)		1.7 ± 0.2	>	0.6 ± 0.0